Investigating Biological Processes at the Single Molecule Level Using Luminescent Quantum Dots

THOMAS PONS[1] and HEDI MATTOUSSI[2]

[1]Laboratoire Photons et Matière, CNRS UPR5, ESPCI, 10, rue Vauquelin, 75005 Paris, France; and [2]Division of Optical Sciences, US Naval Research Laboratory, Washington, DC 20375, USA

Abstract—In this report we summarize the progress made in the past several years on the use of luminescent QDs to probe biological processes at the single molecule level. We start by providing a quick overview of the basic properties of semiconductor nanocrystals, including synthetic routes, surface-functionalization strategies, along with the main attributes of QDs that are of direct relevance to single molecule studies based on fluorescence detection. We then detail some valuable insights into specific biological processes gained using single QDs. These include progress made in probing biomolecular interactions, tracking of protein receptors both *in vitro* and in live cells, and single particle resonance energy transfer. We will also discuss the advantages offered and limitations encountered by single QD fluorescence as an investigative tool in biology.

INTRODUCTION

Semiconductor nanocrystals, or "quantum dots" (QDs), have recently emerged as a new set of fluorophores that can enhance biological assays, fluorescence detection and imaging.[11,45,53,64,65,67,69,93,95,104] This is due to some of their unique optical and spectroscopic properties, which are often not matched by most conventional fluorophores, such as organic dyes and fluorescent proteins. QDs exhibit high fluorescence quantum yields, high photobleaching thresholds, and a pronounced resistance to photo- and chemical-degradation.[45,67,69,95,104] They also exhibit narrow and tunable emission bands along with broad excitation spectra and high extinction coefficient (~10–100 times larger than most dyes). These properties allow the flexibility to excite them efficiently far from their emission peaks. There has been a tremendous interest in using them to develop a variety of biological assays and for sensor design. These include imaging of live and fixed cells, imaging of tissue, immunoassays and energy transfer based assays. Energy transfer based sensing has in particular expanded in the past few years, with sensors developed for the detection of small and large molecule targets, hybridization interactions, and enzyme digestion.[11,53,64,65,67,93,95]

Ensemble measurements are macroscopic in nature and they provide information about average properties of samples such as size, conformation or orientation of proteins. In comparison, single molecule measurements are able to resolve molecular scale heterogeneities and the fate of individual molecules. Fluorescence detection applied to single molecules can allow access to valuable molecular scale information, and it has become one of the most commonly used single molecule techniques in biological research.[18] Furthermore, recent progress in optical instrumentation and the development of highly sensitive detection tools (such as APD and CCD) allowed easier detection and resolution of fluorescence from single fluorophores. This has in turn allowed the development of a variety of single molecule assays to study ligand-receptor binding, changes in the conformation of macromolecules (e.g., proteins, short and large oligonucleotides), and single molecule diffusion and transport.[18,106] Outside biophysical research, single molecule fluorescence was successfully applied to individual colloidal QDs. It allowed access to truly unique and remarkable information about the fluorescence of single QDs that were not accessible from ensemble measurements. In particular, two unique properties distinguish luminescent QDs from most conventional fluorophores: (1) single QD exhibit very narrow PL spectra compared to those averaged for macroscopic samples (FWHM ~ 15 nm vs. 30–40 nm for ensemble spectra at room temperature) and (2) the fluorescence emission of isolated

Address correspondence to Hedi Mattoussi, Division of Optical Sciences, US Naval Research Laboratory, Washington, DC 20375, USA. Electronic mail: hedi.mattoussi@nrl.navy.mil

nanoparticles under continuous excitation is intermittent in nature (blinking).[24,26,49,50,74]

The unique optical properties of QDs can be particularly beneficial for single molecule fluorescence measurements. Due to their large extinction coefficient, narrow emission spectra, and their resistance to photo-degradation, QDs may be individually detected with high signal-to-noise ratios and for extended periods of time (several minutes under sustained irradiation), a feature that is not available to traditional organic dyes. This can permit easy discrimination of different single QD colors. This also makes them particularly suitable for multiplexed single molecule fluorescence imaging. As such, single molecule fluorescence has emerged as one of the major aspects of employing these fluorophores in biology.[16,56]

In this report, we start with a brief description of the most effective synthetic procedures to prepare high quality colloidal nanocrystals, outline the commonly used surface functionalization techniques, and describe the most pertinent photo-physical properties of use to biology. We then review the progress that use of single QD fluorescence has allowed in biology, with a focus on a few representative examples where unique and valuable insights into specific biological processes have been gained. These include progress made in probing biomolecular interactions, tracking of protein receptors *in vitro* and in live cells and single particle energy transfer. We will also discuss the advantages offered and limitations encountered by single QD fluorescence as an investigative tool in biology.

SYNTHESIS, SURFACE-FUNCTIONALIZATION AND PHYSICAL PROPERTIES OF COLLOIDAL QDS

Synthesis of Dispersible and Highly Luminescent QDs

Luminescent QDs that have found most use in biology are colloidal in nature, and they are prepared using solution phase reactions. The first solution-phase growth of the nanoparticles was realized within inverse micelles.[38,90] However, the major advance in solution-phase synthesis took place in 1993, when Bawendi and co-workers showed that "pyrolysis" of organometallic precursors can provide high quality CdSe nanocrystals that have crystalline cores, narrow size distribution (~10% or less) and exhibit relatively high photoemission quantum yields.[71] The first demonstration of this reaction scheme employed the rapid injection of dimethylcadmium ($CdMe_2$) and trioctylphosphine selenide (TOP:Se) mixed with trioctylphosphine (TOP) into a hot (280–300 °C) coordinating solution of trioctylphosphine oxide (TOPO). One of the key aspects of this synthesis route was that colloidal QDs could reproducibly be made to exhibit narrow emission with low defect contributions and relatively high room temperature quantum yields (QY ~ 5–10%). This has allowed performance of several viable photophysical and structural characterizations (using for example absorption, fluorescence spectroscopy and scattering techniques).[61,71,75] It has further raised the potential for technological applications based on QDs (e.g., LEDs and photovoltaic devices).[13,32,43,63,70]

In subsequent studies, Peng and co-workers further refined this reaction scheme and showed that several precursors which are less pyrophoric and less volatile than $CdMe_2$ could potentially be used for preparing high quality colloidal nanocrystals of CdS, CdSe, and CdTe.[80,86] Other groups quickly followed up on Peng's work, and those efforts combined have outlined the importance of impurities (usually acids coordinating to the metal precursors) in the reaction progress. In this route, high purity TOPO and controlled amounts of metal coordinating ligands and metal precursors, such as CdO, Cd carboxylates, phosphonates, or acetyl-acetonates, were used to synthesize various Cd-based nanocrystals, as schematically represented in Fig. 1.[80,86,89] The high temperature synthetic route was also applied to making near-IR emitting PbSe QDs initially by Murray and co-workers, and then by other groups, using oleic acid and Lead(II) acetate trihydrate or lead oxide.[19,72,103,110]

To further take advantage of the progress made in improving the quality of QDs achieved using high temperature synthesis and to improve the luminescence quantum yield, researchers applied the concept of band gap engineering developed for semiconducting quantum wells to the growth of colloidal nanocrystals (see Fig. 1).[48] It was first demonstrated by Guyot-Sionnnest and co-workers that overcoating CdSe QDs with a layer of ZnS could improve the PL quantum yields to values of 30%.[39] Following that two comprehensive reports by Dabbousi *et al.*[15] and Peng *et al.*[79] detailed the complete reaction conditions for preparing a series of CdSe–ZnS and CdSe–CdS core–shell nanoparticles that are strongly fluorescent and stable. We should add that air-stable precursors have also been used for the overcoating reactions, following the reports of synthesis of CdS, CdSe nanocrystals.[54,89] One of the issues associated with overcoating QDs with ZnS shell to improve the PL yield is the crystal lattice mismatch between core and shell materials, which can produce non-homogenous shell structure due to strain-induced defects. To potentially address this problem a few groups have grown multilayer shells on the native core (e.g., CdSe–CdS–ZnS)[105]; this progressively adapts the crystalline lattice parameters of the overcoating shell to those of the core. We should also
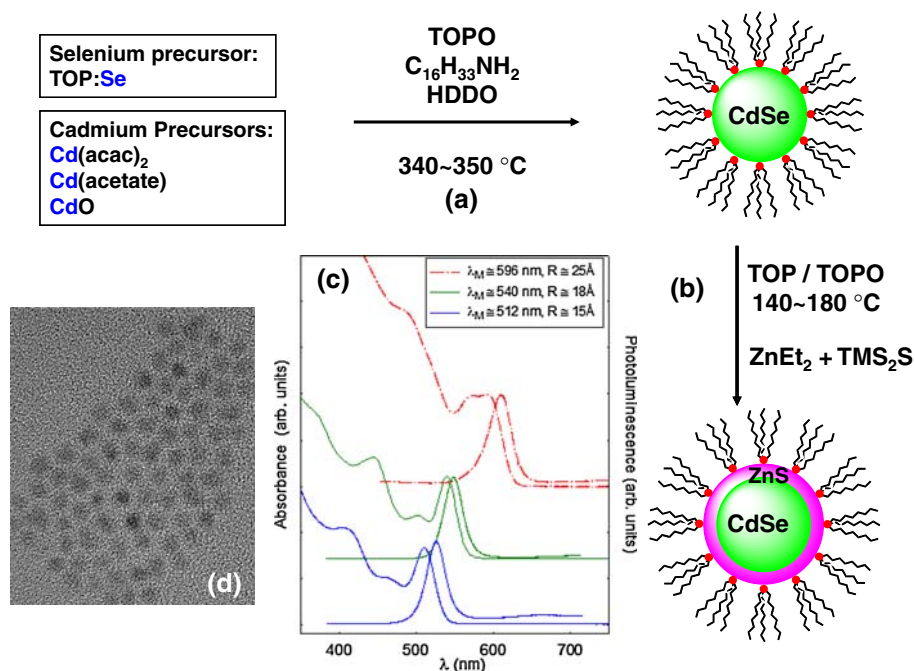
FIGURE 1. (a and b) Schematics of the stepwise synthesis route based on high temperature reaction of organometallic precursors to prepare CdSe–ZnS core–shell QDs. (c) Representative absorption and emission spectra for a set of CdSe core only QDs prepared using the high temperature method. (d) A typical high resolution TEM image of CdSe QDs having a diameter of ~40 Å.

emphasize that QD cores have been synthesized with various materials combinations, including II-VI (e.g., CdSe, CdS, CdTe, ZnSe…) and III-V (e.g., InP, InAs…) semiconductors and their alloys.[77] However, thus far only CdSe-based QDs have provided both low size dispersity and high QYs; these have been used in all single QD studies presented in this review.

Water-Solubilization Strategies

Since publication of the first reports on developing colloidal QDs as biological labels, several strategies aimed at developing stable water dispersions of luminescent QDs have been developed. These strategies can be loosely divided in two main categories: ligand-exchange and encapsulation within block copolymers or phospholipid micelles (see Fig. 2).

Ligand Exchange

Water-solubilization via ligand exchange involves replacing the native hydrophobic surface ligands (mainly TOP/TOPO) with bi- and/or multi-functional hydrophilic ligands. The hydrophilic ligands are made of metal-coordinating anchor group(s) (often thiol-based groups) at one end for binding to the nanocrystal surface. At the other end the ligands present hydrophilic groups (such as carboxyl or poly(ethylene glycol)) that promote affinity to aqueous solutions.

Water-transfer via cap-exchange with small ligands has been attempted by several groups in the past decade, because of its ease of implementation and the commercial availability of several of these ligands. A benefit of this strategy is that the resulting hydrophilic QDs are compact in size,[85] a property that can be extremely important for applications such as intracellular transport.[67] However, the stability of the resulting QDs in buffer solutions is often poor. For instance, thiol-alkyl-carboxyl ligands (including mercaptoacetic acid MAA, and mercapto-undecanoic acid, MUA) produce nanocrystals that tend to progressively aggregate in physiological conditions within a relatively short period of time. A concomitant decrease in the fluorescence quantum yield is also measured. This is most likely due to desorption of the ligands from the QD surface. Peng and co-workers attempted to resolve this problem by preparing hydroxyl-terminated dendron ligands that were also end-functionalized with thiol groups to promote anchoring on the QD surface, then later used amine-terminated dendrimers for cap exchange; the latter allowed cross-linking of the ligands to form "dendron-boxed" QDs.[33,101] To address the long-term stability of QDs prepared via cap-exchange our group relied on the use of bidentate thiol ligands such as dihydrolipoic acid (DHLA).[62] However, most of the commercially available thiol-terminated ligands (MAA, MPA, MUA as well as DHLA) rely on the deprotonation of the carboxyl
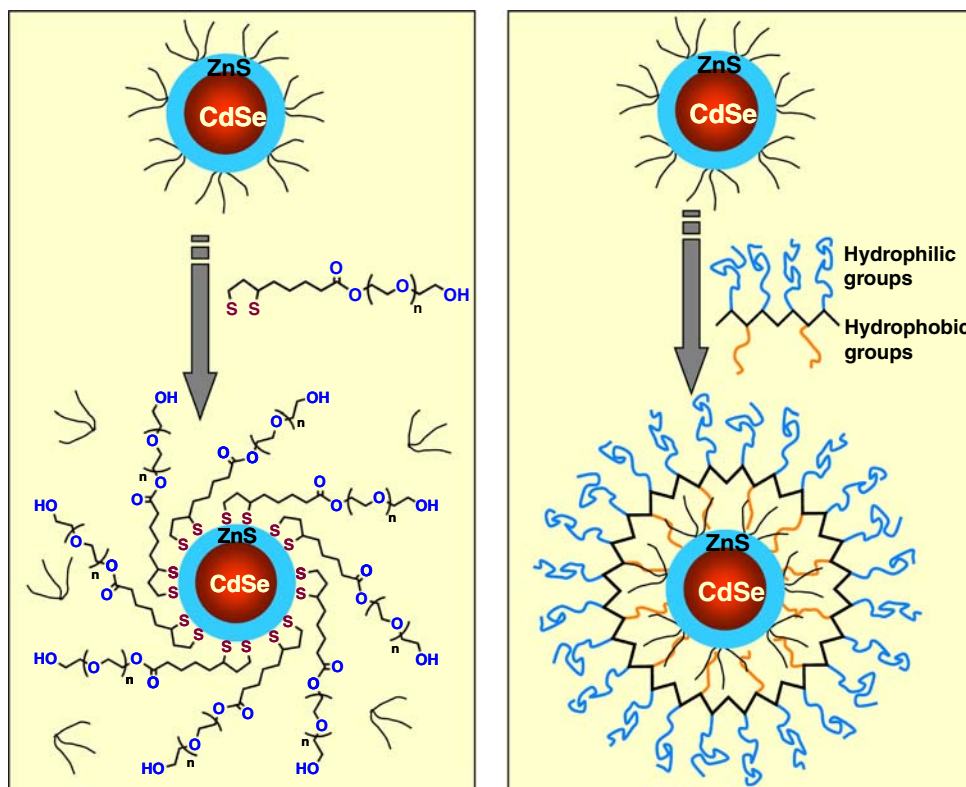
FIGURE 2. Schematics of the two main strategies used for surface-functionalization and transfer to water of colloidal QDs used to-date. (Left) Representative example of the cap exchange strategy using polyethylene glycol-appended dihydrolipoic acid (DHLA–PEG). (Right) Encapsulation within an amphiphilic block copolymer.

groups terminal groups to achieve dispersion in water, and this has limited one's ability to prepare homogeneous QD dispersions at acidic pHs.[62] We have recently developed a new set of DHLA ligand derivatives that can potentially allow one to overcome these constraints/limitations. This relied on appending poly(ethylene glycol) (PEG) segments with variable chain-lengths onto dihydrolipoic acid.[68,99] QDs capped with DHLA–PEG ligands are well dispersed in aqueous media and stable over an extended period of time and over a relatively broad pH range. Subsequently, we demonstrated that inserting reactive groups at the lateral end of the DHLA–PEG ligand (such carboxyl or amine) could permit easy implementation of known coupling reaction to attach QDs to proteins and peptides.[58,96,97] With the ligand exchange strategy, the nature of the anchoring group to the QD surface (e.g., monodentate vs. multidentate) can seriously affect the long-term stability of the hydrophilic QDs.

In a somewhat different rationale, Weiss and co-workers have used phytochelatin-related peptides terminated with a few cysteine groups for anchoring on the QDs.[81] This clever strategy also relies on the multidentate thiol interactions with the inorganic surface of the nanocrystals, which improves the stability of the

ligand/QD system. Moreover, using peptides as the actual ligands can potentially allow direct biological targeting. Rather large amounts of peptide ligands are needed to carry out an effective cap exchange, because this process naturally requires a large excess of ligands.

In a few recent studies, amine-rich polymers have been employed to functionalize the QD surfaces, and it has been proposed that for these polymers, water transfer to aqueous media is realized via cap exchange of the native ligands. Systems used include amphiphilic hyperbranched polyethyleneimine,[73] poly(ethylene glycol)-grafted polyethylenimine,[20] and poly(ethylene glycol-b-2-N,N-dimethylaminoethyl methacrylate) (PEG-b-PDMA) diblock copolymer.[100] Cap exchange with thiol-terminated silane ligands, followed by further cross-linking to form a silica shell coating was also utilized as a means to promote hydrophilicity of CdSe–CdS(ZnS) core–shell nanocrystals.[6,30]

Encapsulation within Block Copolymers and Phospholipid Micelles

This strategy relies on the use of bifunctional amphiphilic polymers having hydrophobic segments, which selectively interact (and interdigitate) with the

native TOP/TOPO shell, and hydrophilic units that promote QD dispersion in aqueous media.[28,57,78,104,109] In general achieving a controlled balance of hydrophobic and hydrophilic blocks within the polymers is necessary for its ability to promote water solubility of the QDs. In one of the early uses of this strategy, Wu *et al.* used a block copolymer shell consisting of 40% octylamine-modified polyacrylic acid.[104] Pellegrino *et al.* used poly(maleic anhydride alt-1-tetradecene) for QD encapsulation.[78] Following adsorption on the TOP/TOPO QDs, further addition of bis(6-aminohexyl) amine formed cross-linked polymers on the QDs, and subsequent hydrolysis of the unreacted anhydride units was shown to make the QDs water soluble.

The second encapsulation method employed phospholipid derivatives which formed micelles. In particular, the first demonstration of this strategy was reported by Dubertret and co-workers who used phospholipids containing 40% 1,2-dipalmitoyl-*sn*-glycero-3-phosphoethanolamine-*N*-[methoxy(polyethylene glycol)-2000] (mPEG-2000 PE) and 60% of 1,2-dipalmitoylglycero-3-phosphocholine (DPPC) to carry out encapsulation of CdSe–ZnS QDs and their transfer to buffer solutions.[21,27] This technique is simple to implement as most phospholipids are commercially available, and like polymer encapsulation can yield water-soluble QDs with QYs higher than those obtained via ligand exchange. This strategy has some of the stability issues at very low concentrations encountered by micelles in general. In addition, it is

possible that more than a single nanocrystal could be contained within each micelle; nonetheless, it has been recently shown that these can be removed using ultracentrifugation or high pressure liquid chromatography.[7] Overall one of the constraints of using encapsulation is that the overall hydrodynamic size of the nanoparticles becomes inevitably large.

Photo-Physical Properties of Colloidal QDs

Semiconductor QDs are neither wholly atomic nor bulk semiconductors; instead they are nanoscale assemblies of atoms (100–1000 s depending on the size). The spatial confinement of intrinsic electron and hole carriers to the physical dimensions of the nanocrystal (quantum confinement effects) imparts on these materials novel electronic properties not exhibited by their bulk parent materials or individual atoms/molecules. These confinement effects manifest when the nanocrystal size becomes comparable to, or smaller than, the bulk Bohr exciton radius.[29,47] The best known and understood confinement effect is the widening of the energy band gap with decrease of nanocrystal size. This manifests itself as a blue shift of the first absorption peak and the photoluminescence maximum with decreasing particle size, along with the appearance of discrete energy states in both the valence and conduction bands. It also manifests in the appearance of tunable (by size and composition) photoemission properties, as shown in Fig. 1 for CdSe-based QDs and Fig. 3 for other QD
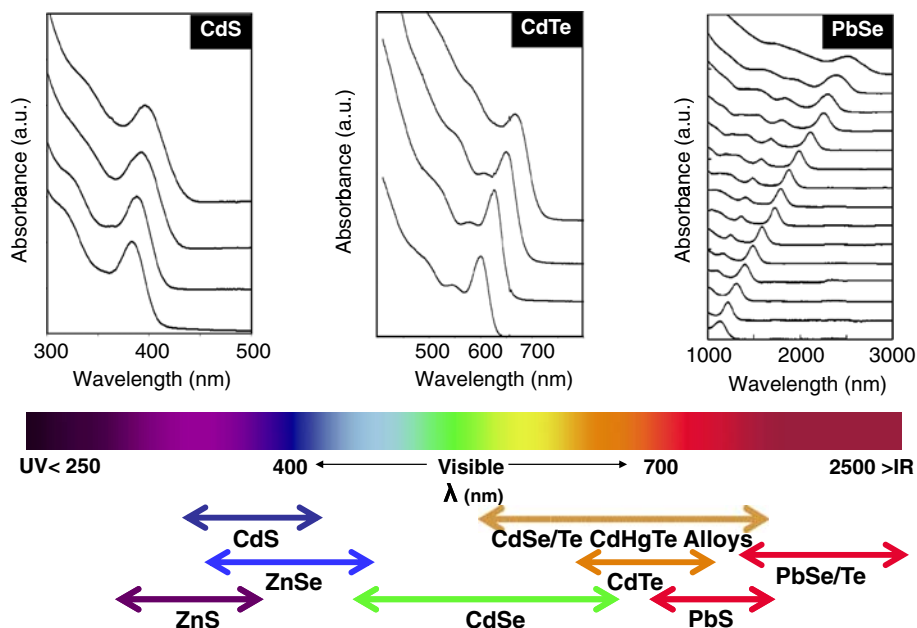
FIGURE 3.   (Top) (Top) Representative absorption spectra for CdS, CdTe, and PbSe QDs prepared using high temperature solution reaction. The shift in the position of the first absorption peak reflects increase in the nanocrystal size. (Bottom) PL emission windows for various II–VI, III–V and hybrid "III–VI" core materials. Figures partially reproduced from Medintz *et al.*,[67] Peng and Peng,[80] and Yu *et al.*,[110] with permission from the American Chemical Society and NPG.

materials. Resolution in the excited state energy levels and separation between the valence and conduction band levels depends on the width of the nanocrystal size distribution and the type of semiconducting materials used.

In addition to the size and composition dependent optical and spectroscopic properties, colloidal luminescent QDs have another characteristic that distinguishes them from organic fluorophores: intermittent photoemission (blinking) of individual nanocrystals. The photoluminescence of isolated QDs displays an alternation of "on" (emitting) and "off" (dark) periods, which durations follow a "heavy-tail" power law distribution with time.[49,50,74] This implies that individual QDs can experience dark periods, where no emission can be collected. This feature is especially important for single molecule detection, as a QD can periodically "disappear" from the observation field. PL blinking of single QDs has attracted much interest, because its underlying mechanisms are not fully understood.[50] Two recent studies have shown that CdSe QDs coated with thick CdS shells can exhibit a drastic reduction in the blinking rate.[10,59] One may expect that these improvements will soon produce QD probes that are better suited for biologically relevant single molecule studies. These properties combined with the high quantum yields realized for core–shell QDs and the very high extinction coefficient constitute the most important properties for use in biology.

Finally, the size of a QD varies from ~10 to ~50 nm, depending on the type of solubilization technique used.[67,85] It is larger than organic fluorophores but comparable to that of fluorescent proteins. The relatively large size allows the ability to conjugate several biomolecules on the surface of a single QD, which can be advantageous in certain instances. Enhanced target affinity and higher rates of energy transfer can be realized with multifunctional QD-conjugates. However, the large size of hydrophilic QDs and their conjugates can influence their diffusion in biological media and may affect their ability to access certain cellular compartments. In addition, multivalency may be a limitation in instances when a strict one-to-one QD–biomolecule conjugation is required.

It should be noted that despite the progress made in designing reproducible techniques to achieve the effective transfer of luminescent QDs and an array of other inorganic nanoprobes to buffer media, there are still several issues associated with the use of QDs in biology. These issues stem from problems such as limited temporal stability to changes in pH for several nanocrystals prepared using cap exchange with mono-thiol-alkyl-COOH ligands and some of the polymer encapsulation approaches developed in the past decade. The limited pH stability can often produce nanocrystals that experience aggregation build up in live cells and in blood. pH limitation in general stems from sensitivity of the capping/encapsulating layer used to promote hydrophilicity of the final nanocrystals. Insertion of PEG oligomers have alleviated some of these issues in some of the latest studies.[58,96,97,109] The wide range of size variation of hydrophilic QDs has also been a serious problem for applications requiring compact nanocrystals and their conjugates. Batch to batch variation of commercially available QDs have also been reported in various studies. There have been sustained efforts by several groups to address these problems and eventually produce nanocrystals that can allow one to take advantage of some the unique properties of these probes.

SUMMARY OF SOME OF THE PROGRESS MADE USING QDS FOR ENSEMBLE MEASUREMENTS

There has been an array of biological assays developed in the past 8 years where researchers have tried to exploit the unique properties of luminescent QDs. These developments can essentially be summarized in three areas: use for live cells imaging where easy to implement multiplexing capabilities, slow degradation and high photo-bleaching threshold were demonstrated. These range from multicolor labeling of fixed cells using QD–antibody conjugates, investigating specific biological processes that require extended observation, to probing membrane specific processes such as T cell stimulation.[2,21,45,87,104] The very high two-photon action cross-section of QDs has been effectively used to realize deep tissue imaging with reduced IR excitation and very weak auto-fluorescence contribution.[51] In somewhat similar rationale, one-photon fluorescence of NIR emitting QDs was also used to carry out real time mapping of sentinel lymph nodes in live animals during surgery, where nodes as deep inside the tissue (~100 mm–1 cm deep) were imaged in real time using relatively low excitation intensity.[46] Use of QDs for in vitro sensor development based on fluorescence detection and energy transfer has also witnessed a substantial development. They have been used for single and multiplexed immuno-sensing of soluble toxins.[31] Energy transfer based assays have been used to detect DNA hybridization, recognition of full enzymes by QD–aptamer conjugates,[53] enzyme cleavage of peptides,[65,93] and glycosylation levels in proteins.[76]

USE OF SINGLE QDS FOR THE *IN VITRO* DETECTION OF BIOMOLECULAR INTERACTIONS

Because of the very narrow PL spectrum of individual QDs, the proportion of photons that are rejected by the narrow band detection filters is substantially reduced, and this simplifies the spectral deconvolution of signals from different QD colors. This could enhance the signal-to-noise ratio and can be very beneficial to single molecule assays, where the number of detected photons is inherently low. The ability to resolve single QD emission for extended periods of time will undoubtedly allow higher detection sensitivity and data collection over long time intervals.

Co-Localization of Distinct QD Probes

This configuration has been used to develop multiplexed assays, where interactions (and binding) of two QD-bioconjugates emitting at different spectral windows to different sites on the same target molecule can be simultaneously detected. A typical example can involve two distinct emission QDs conjugated to two different DNA probes, mixed in a solution with a target oligonucleotide that contain complementary sequences for both probes. The target DNA hybridizes simultaneously with the two QD–DNA conjugates (dual hybridization). If immobilized on a substrate, this dual hybridization could then be detected optically using wide field fluorescence microscopy, where the signals from the two QD probes are simultaneously imaged.

Wang and co-workers[40] applied this strategy to carry out a genetic analysis of anthrax "pathogenicity." In general, a positive identification of this bacterium requires the simultaneous detection of three distinct genes, namely rpoB, pagA, and capC in the same sample. Three pairs of target-specific DNA probes were conjugated (combinatorially) to three distinct color QDs emitting at 525, 605, and 705 nm, respectively. As targets, they used three synthetic oligonucleotides, each derived from conserved sequences from each of the three anthrax-related genes; these were used as simulated targets (in a background of *E. coli* genomic DNA) for analysis. They first used the simultaneous fluorescence signals in the combined pseudocolors of the spots, namely, indigo, magenta, and orange, as an indication of the presence of rpoB, pagA, and capC, respectively (Fig. 4a). They then carried out four sets of experiments, where the specificity of the assay was
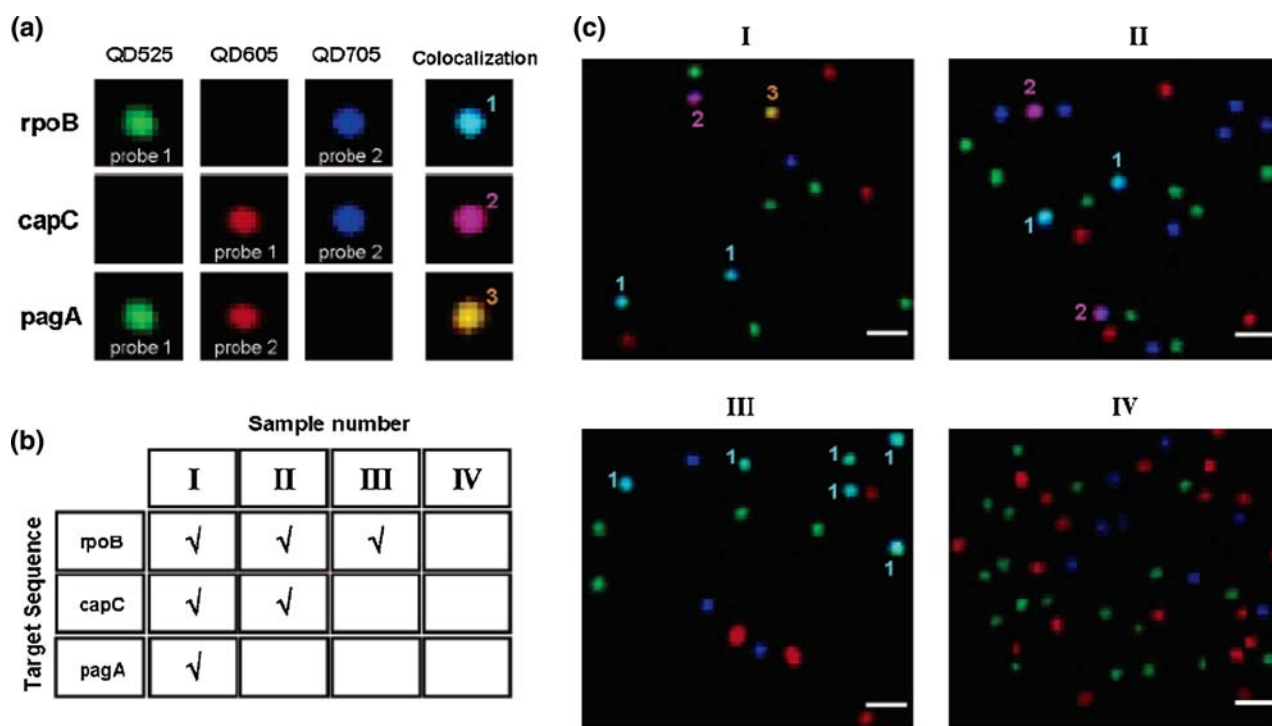

FIGURE 4. Simulated multiplexed analysis of anthrax-related genetic targets: (a) color set for the three pairs of target-specific QD nanoprobes and their resulting co-localized fluorescent images upon hybridization. (b) Four samples containing different combinations of the three targets, rpoB, capC, and pagA. Checks represent the existence of certain target sequences. Sample IV is the negative control. (c) Fluorescent images I, II, III, and IV correlate with samples I, II, III, and IV, respectively (Bar dimension is 1 μm). Figure partially reproduced from Ho *et al.*,[40] with permission from the American Chemical Society.

essentially defined by its capacity to correctly identify and quantify the individual target sequences in a complex mixture of various target combinations (Fig. 4b). In the first step, fluorescent spots in all the three combined pseudocolors were detected, which indicated the presence of the three targets in the solution (Fig. 4c, I). In the next two experiments, they found that the presence of two (Fig. 4c, II) or only one (Fig. 4c, III) target could also be unambiguously determined (i.e., without false positive or negative). In the fourth negative control sample, only fluorescent spots stemming from unhybridized blue, green, and red QD probes were observed (Fig. 4c, IV); in this sample no specific target was present. A similar assay has been reported using QD–antibody conjugates binding different sites of the same target protein.[1]

Alternatively, the conjugate dispersion could be injected into a small glass capillary and the QD signals could be detected sequentially as the conjugates pass through the observation volume. In both cases, the presence of the target could be inferred from the co-localization of two distinct single QD emission signals, because the size of the total target–DNA probe–QD complex is smaller than the optical resolution of the detection system. This solution-phase method is fast (solution vs. surface immobilized reagents) and does not require separation of unbound probes; these are usually not co-localized. It allows identification of samples without prior polymerase chain reactions (PCR) amplifications, which are not quantitative and can introduce non-negligible errors. It also allows detection of low abundance targets and has a higher sensitivity than microbead assays in which weak target signals may be difficult to discriminate against the strong microbead coding signal. The sensitivity of this assay format has been demonstrated even in the presence of a strong nonspecific background (i.e., samples mixed with cell extracts).[1]

Other reported assays using this format included QD-conjugate binding two extremities of individual DNA molecules that were stretched on a glass surface, and the identification of single large entities such as viruses or bacteria from different strains in a macroscopic mixture.[14,23,36] These assays often use QDs with spectrally distinct emissions conjugated to different antibodies. In the virus constructs, the collected fluorescence signal (being a mix of signals emitted by different QD–antibody conjugates bound onto a single scaffold) provided a spectral "bar code" that accounted for the nature and number of specific proteins displayed on the virus surface. This has for example allowed a rapid identification of the virus strain.[1]

We should emphasize that these assay formats, such as the one used for virus identification could be performed with organic fluorophores. However, comprehensive analysis requires the usual complex spectral deconvolution and tedious data analysis. In comparison, QDs offer advantages such as higher sensitivity and spectral unmixing (deconvolution), which enable the multiplexed detection of single small biomolecules carrying only a few fluorescent markers. Nonetheless, the limitation of assays based on QD fluorophores, derives from the intermittent emission of single QDs. This can cause a fraction of the co-localized QD probes to occasionally appear as isolated QDs, which may introduce "false negative" counts.

Co-Localization Studies Using QD–Dye Pairs

The same concept was applied by Webb and co-workers to investigate the relationship between ensemble fluorescence quantum yields measured for macroscopic samples and the blinking properties of individual QDs.[107] The authors coupled Streptavidin-functionalized 525-nm emitting QDs with biotin-functionalized Alexa Fluor 594 dye and used the fluorescence collected from dot and dye to distinguish between dark and bright freely diffusing single nanocrystals. This presents a different configuration from that of surface-immobilized QDs (e.g., dispersed in polymeric films). The bright fractions of QDs were measured by fluorescence coincidence analysis and two-photon fluorescence correlation spectroscopy. In particular, they reported that the bright fraction of QDs was proportional to the measured macroscopic quantum yields of the samples. However, brightness of individual QDs was constant across samples with different quantum yields. They then applied the same measurements to solutions with much higher viscosity, where nanocrystal residence time in the illuminated volume was substantially increased. Their findings clearly indicated that increasing the residence time by as much as 10-fold did not change the fraction of "apparently dark" QDs, which they attributed to the presence of two populations of QDs in a sample: one dark non-emitting and one emitting; only the emitting fraction contributed to the measured macroscopic fluorescence yields. These results may be very informative, as they can potentially provide correlation between ensemble quantum yield and single molecule fluorescence; additional work is still needed to better understand the correlation between the fluorescence properties of single and ensemble QDs.

SINGLE PARTICLE ENERGY TRANSFER

Fluorescence Resonance Energy Transfer (FRET) involves the non-radiative transfer of excitation energy from a fluorescent donor to a ground state proximal

acceptor. It is governed by the dipole–dipole interaction (Förster) mechanism, which results in a strong dependence of the transfer efficiency, E, on the donor–acceptor separation distance, r ($E \sim 1/r^6$) and on the spectral overlap between the donor emission and the acceptor absorption. Because of the strong dependence of the transfer efficiency on separation distance, this technique provides a unique tool to probe intermolecular association and intra-molecular conformational changes in the 1–10 nm range.[17,34] FRET provides a powerful means for studying biomolecular interactions involved in drug screening or disease diagnosis. It has been widely used for studying changes in protein and oligonucleotide conformation *in vitro* and in live cells using dye donor–dye acceptor FRET pairs. It has been shown in the past 5 years that QDs offer a few unique advantages (compared to organic dyes) for use as FRET donors.[11,12,66,84,94] As demonstrated for ensemble measurements, some of the size-tunable absorption and emission properties can be very beneficial to implementing single particle energy transfer. The broad absorption spectra of QDs allow excitation of the donor far from the acceptor absorption peak, which substantially reduces direct excitation contribution to the acceptor signal. In addition, the narrow emission of single QDs can be tuned to match the acceptor absorption spectrum.[12] This narrow emission also allows easy deconvolution of the donor and acceptor emissions. Finally, because a QD can be conjugated to several acceptors, the overall FRET rate can be substantially increased, a clear advantage especially with longer separation distances. Following the success in using QDs as energy transfer donors in ensemble assays, there has been a natural desire to translating these assays to the single molecule level. This can allow access to single molecule information, reduces materials consumption, while potentially allowing higher sensitivity to be reached.

Single particle/molecule (sp- or sm-) FRET can use either surface-immobilized or freely diffusing QDs and QD-bioconjugates. Probing immobilized QD-assemblies can allow one to collect and resolve time-dependent conformational changes at the single molecule level. In this configuration one plots time-traces of donor and acceptor emission profiles, and changes of these profiles are used to account for alterations in the FRET interactions. However, spFRET using surface-immobilized assay remains difficult to implement, due among others to weak FRET efficiency (in particular, for one QD–one dye pairs), a feature associated with some of the commercial nanocrystals; these often require multi-layer functionalization and additional conjugation steps.[67] Moreover, the intermittent nature of single QD emission prevents one from quantitatively monitoring variations in the FRET efficiency with time.

Finally, interaction of the QD-bioconjugate with the surface may alter the biomolecule conformation and its behavior.

Probing freely diffusing QD-bioconjugates in solution samples can allow one to circumvent some of the issues encountered with immobilized conjugates, by for example limiting the specimen excitation to the residence time within the illuminated volume. It also reduces issues associated with intermittent emission and data collection and analysis. Solution-phase single particle FRET configuration utilizes confocal microscopy combined with a highly focused laser beam for specimen excitation, two dichroic mirrors and two highly sensitive detection systems (Fig. 5a). The collected signal consists of simultaneous bursts of PL intensities from the donor (QD), collected on the donor channel, I_D, and the acceptor (dye), collected on the acceptor channel, I_A, corresponding to Brownian diffusion of single QD conjugates in and out of the confocal volume. In practice, the spFRET signature consists of plotting the population fraction of events (or simply the number of events) vs. emission ratio, η, defined as $\eta = I_A/(I_A + I_D)$; η is also be referred to as the spFRET efficiency, E. For a control solution containing QD donors only, the population fraction vs. η (or number of events vs. E) is reduced to a peak centered at $\eta = 0$ (or $E = 0$), due to absence of FRET. For samples containing QD–dye pairs, non-zero contribution from the acceptors due to energy transfer broadens the distribution peak and shifts it to higher η values (Fig. 5).[84]

In what follows we will describe a few representative examples where single particle FRET applied to QDs used to provide valuable and unique information about the dynamics of Holliday junction, spectrally resolved FRET, the detection of target DNA sequence and the heterogeneity in QD–protein bioconjugates. In these examples, either surface-immobilized or solution-phase configurations were employed.

### spFRET of Immobilized QD–Oligonucleotide and QD–Protein Conjugates

We describe two recent examples. In the first, single immobilized QD–oligonucleotide conjugates were used to probe the dynamics of DNA Holliday junctions.[41] One of the characteristics of this four DNA strand assembly is that its conformation fluctuates between two different forms depending on salt concentration. For example, in the absence of multivalent ions and at low salt concentration, the junction has an open configuration. At high salt concentration, effects of electrostatic repulsions are reduced and the junction folds into one of two-stacked conformers. The authors used streptavidin–QDs which were first immobilized on a
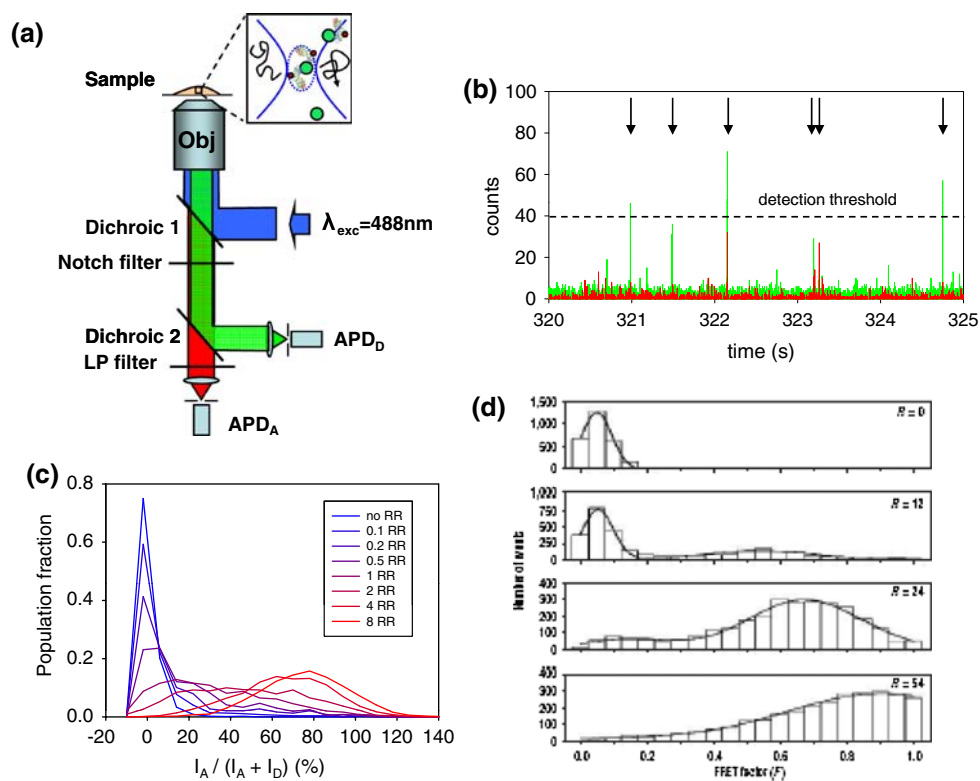
FIGURE 5. (a) Confocal microcopy set up used for implementing solution-phase spFRET. (b) A typical example of superimposed donor (green) and acceptor (red) time traces. Only bursts with the sum of both signals exceeding the threshold level (indicated by arrows) are used for analysis. (c) Emission ratio distributions obtained from spFRET measurements as a function of the acceptor-to-QD ratio. (d) Emission events vs. efficiency *E* reported in Zhang *et al.*[114] Figure partially reproduced from Pons *et al.*[84] and Zhang *et al.*,[114] with permissions from the American Chemical Society and NPG.

glass substrate using biotinylated BSA. First, they exposed the immobilized QDs to solution of double stranded DNA sequence having one end labeled with biotin while the other end carries a Cy5 dye to promote the formation of surface-tethered QD–Cy5 pairs. This experiment was used to demonstrate that blinking of individual QDs is indeed temporally correlated with that of the dye only when surface-immobilized QD–streptavidin–DNA–Cy5 conjugates were formed, i.e., FRET interactions were present. Through an alternation between green laser excitation (able to excite the QD–dye pair) and red laser excitation (which excites the dye only), they showed that FRET interactions could be eliminated by bleaching of the dye under sustained red light excitation, which rendered the dye acceptor inactive and unable to interact with the QDs; after dye recovery correlation between the blinking of QD and Cy5 emissions could again be detected.[41] They then applied this technique to explore the dynamics that characterize DNA Holliday junction, which was assembled from four single stranded DNA molecules, two of them were unlabeled, one pre-labeled with biotin and the other labeled with Cy5 acceptor (see schematics in Fig. 6). Experiments were carried out at pH 7.5 in Tris:HCl buffer where conformational transition between the two states are slow enough to allow resolution on a CCD camera (~100 ms). They found that a small fraction of the QD fluorescence showed anti-correlated "two-state" fluctuations between the QD signal and that of the Cy5 dye, with both states exhibiting significant acceptor contributions. The behavior was different from the one observed when unconjugated QDs are probed (in the same sample), where no alternation in the blinking pattern was measured. They confirmed that this characteristic behavior is similar to the case where a Cy3–Cy5 pair was used instead (see Fig. 6 and Hohng and Ha[41]). They further confirmed their observation by carrying out dwell time analysis of high and low FRET states using QD–Cy5 and Cy3–Cy5 pairs and found that there is a good agreement in dwell time of the high and low FRET sates collected from both pairs, even though the system using QDs allowed a much larger total number of transitions to be observed. These finding clearly confirm that conformational changes in the Holliday junction induce fluctuations in the FRET efficiency measured between the QD and dye at the single molecule level.
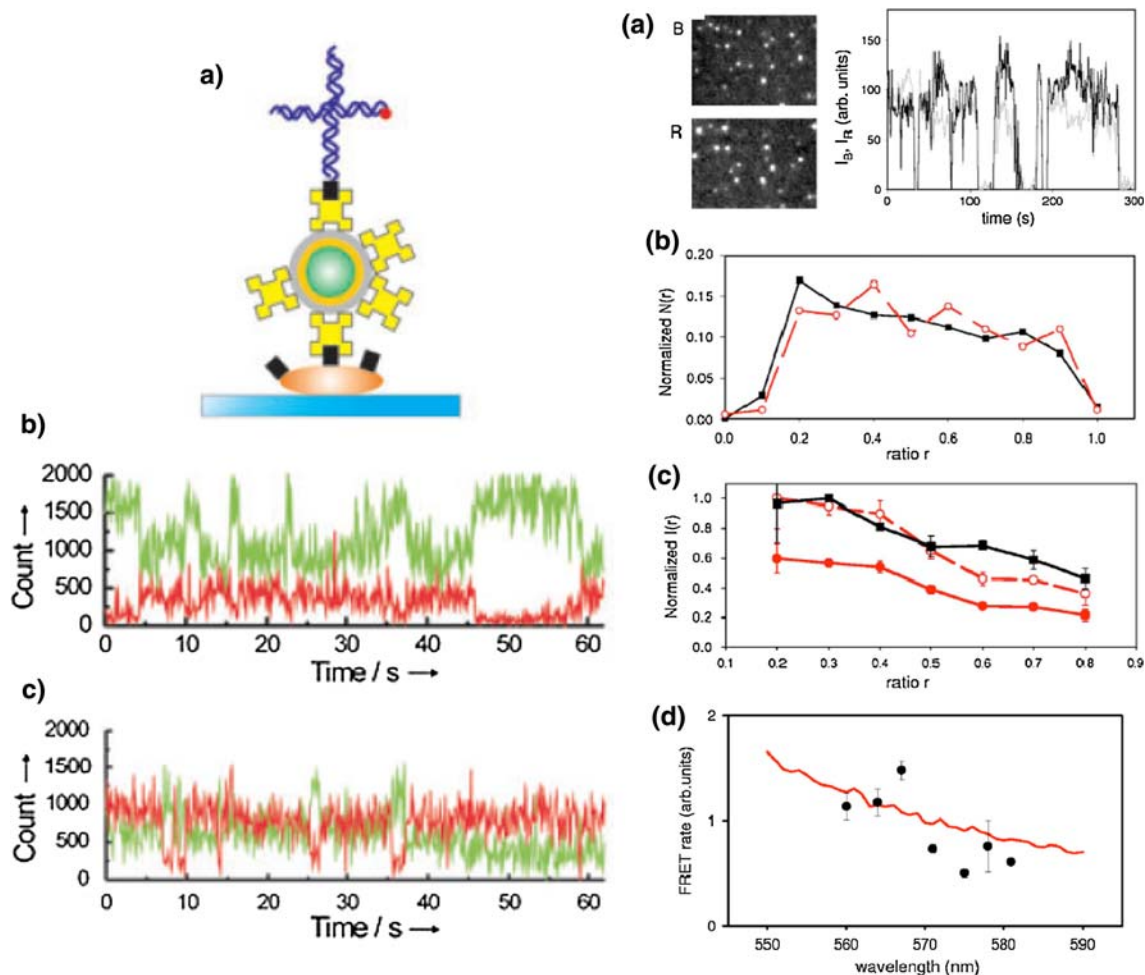
FIGURE 6. (Left panel) Single-pair FRET between 585-nm QDs and Cy5 bound via a Holliday junction. (a) Schematics of the junction assembled on the immobilized streptavidin–QD via biotinylated BSA. (b) Time-traces collected from some of the assemblies showing anticorrelated fluctuation in the signals of QD and Cy5. (c) Similar traces for Cy3–Cy5 pair used for the same junction. (Right panel) (a) Simultaneous PL images on the blue B and red R sides of the dichroic showing a few 575 nm QD–MBP conjugates. I_R black and I_B gray intensity traces of a QD exhibiting $r \sim 0.45$. (b) Population distribution of QDs conjugated to MBP (squares) and QXL520–MBP (open circles) vs. r. (c) Average intensities of single QDs conjugated to MBP (squares) or to MPB–QXL520 (filled circles) vs. emission ratio r. The normalized intensity distribution I/I_{max} for QD–MBP–QXL520 is shown for comparison (open circles). (d) Direct comparison between the wavelength-dependent FRET rates from steady-state (solid line) and single QD measurements (circles) for the QD–QXL520 pair. A total of 220 single QD traces for the QD–20 MBP and 310 single QD traces for the QD–20 MBP–QXL520 were used. Data reproduced from Hohng et al.[41] and Pons et al.,[83] with permission from Wiley–VCH and AIP.

In the second example, our group applied spFRET to immobilized QD–protein–dye conjugates to confirm the presence of spectrally resolved energy transfer observed for ensemble measurements.[83] Spectrally resolved FRET is a unique property of QDs and is due to a combination of broad dye absorption and narrow single QD emission. Indeed, an ensemble PL spectrum is composed of the sum of very narrow single QD spectra. This produces distinct single QD spectral overlap with the acceptor absorption spectrum, resulting in an apparent wavelength-dependent FRET efficiency. We measured the intensities and emission wavelengths of single QDs from a 575-nm centered population, conjugated to 20 proteins that were either unlabeled or labeled with a QXL520 (quencher) and immobilized on a glass cover slip. The QD PL coincides with the red shoulder of the dye absorption. To determine the position of each QD emission, the fluorescence image was split into two windows using a dichroic mirror centered at 570 nm. Three QD fractions could be detected, one emitting in the red window, one emitting in the blue window of the dichroic, while a third having emission around 570 nm leaked into both channels (Fig. 6). The QD signal from each window identified as blue I_B and red I_R components, while an emission ratio $r = I_B/(I_B + I_R)$, was used to
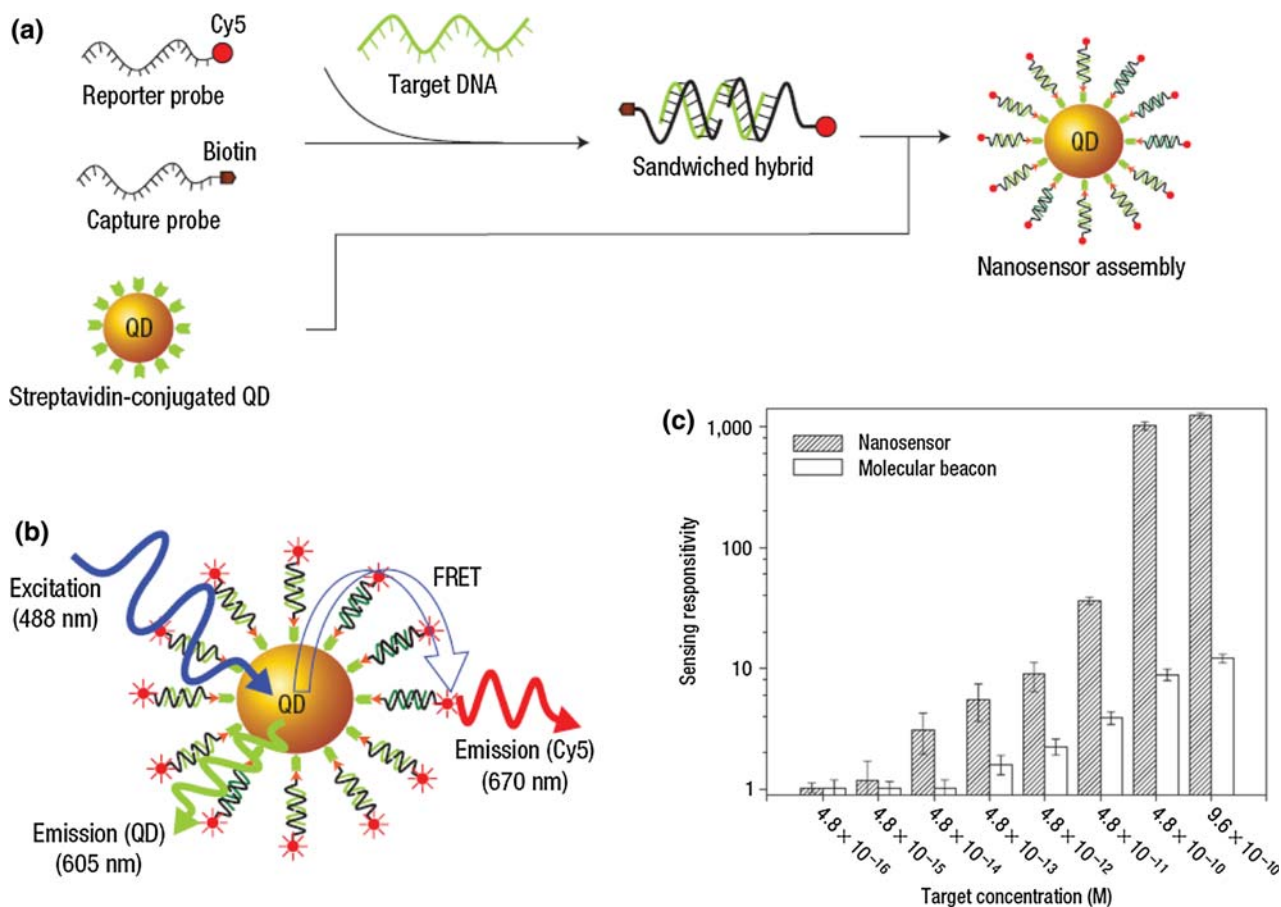
FIGURE 7. Schematic of single-QD-based DNA assemblies. (a) Conceptual scheme showing the formation of a sensing assembly in the presence of targets. (b) Fluorescence emission from Cy5 on illumination on QD caused by FRET between Cy5 acceptors and the QD donor the assembly. (c) Sensing responsivity at different target concentrations for nanosensors and molecular beacons. Reprinted with permission from NPG[114].

determine the QD central emission, e.g., $r = 0.5$ corresponds to a 570-nm QD whereas higher and lower values indicate bluer and redder QDs, respectively. Two histograms were constructed, one for the population distribution as a function of the ratio r, $N(r)$, by counting the fraction of QDs exhibiting a particular r value, the other for the average intensity $I = I_B + I_R$ vs. r. Figure 6 shows that the population distribution $N(r)$ was the same for QDs conjugated to labeled or unlabeled MBP, with an average emission ratio of 0.50. There was, however, a significant change in the shape of the intensity distribution I vs. r, with bluer QDs exhibiting higher quenching than the redder counterparts (Fig. 6, right panel c). This reflects weaker spectral overlap of the "redder" QDs with the dye than their "bluer" counterparts. A FRET rate spectrum was extracted from the ratios between the two intensity distributions in the absence and presence of the acceptors, and compared to the one derived from the steady-state experiments. These data also showed that

the single QD and solution ensemble experiments were consistent (see Fig. 6). This heterogeneity should always been taken into account when analyzing single QD FRET data.[83]

Solution Phase spFRET Applied to DNA Hybridization

In the first demonstration of solution-phase spFRET with QDs Zhang *et al.* applied the technique to DNA hybridization and showed that it could allow detection of a target sequence with high sensitivity (Fig. 7).[114] Their reagents included a "reporter probe" labeled with an organic dye acceptor, a biotinylated "capture probe" and streptavidin–QDs (SA–QDs from Invitrogen). The probes were designed to have complementary sequences to two different regions of the target sequence; thus simultaneously hybridization of the two probes with the target DNA can take place if the latter is present. They first mixed the two probes with the DNA target, which resulted in the formation
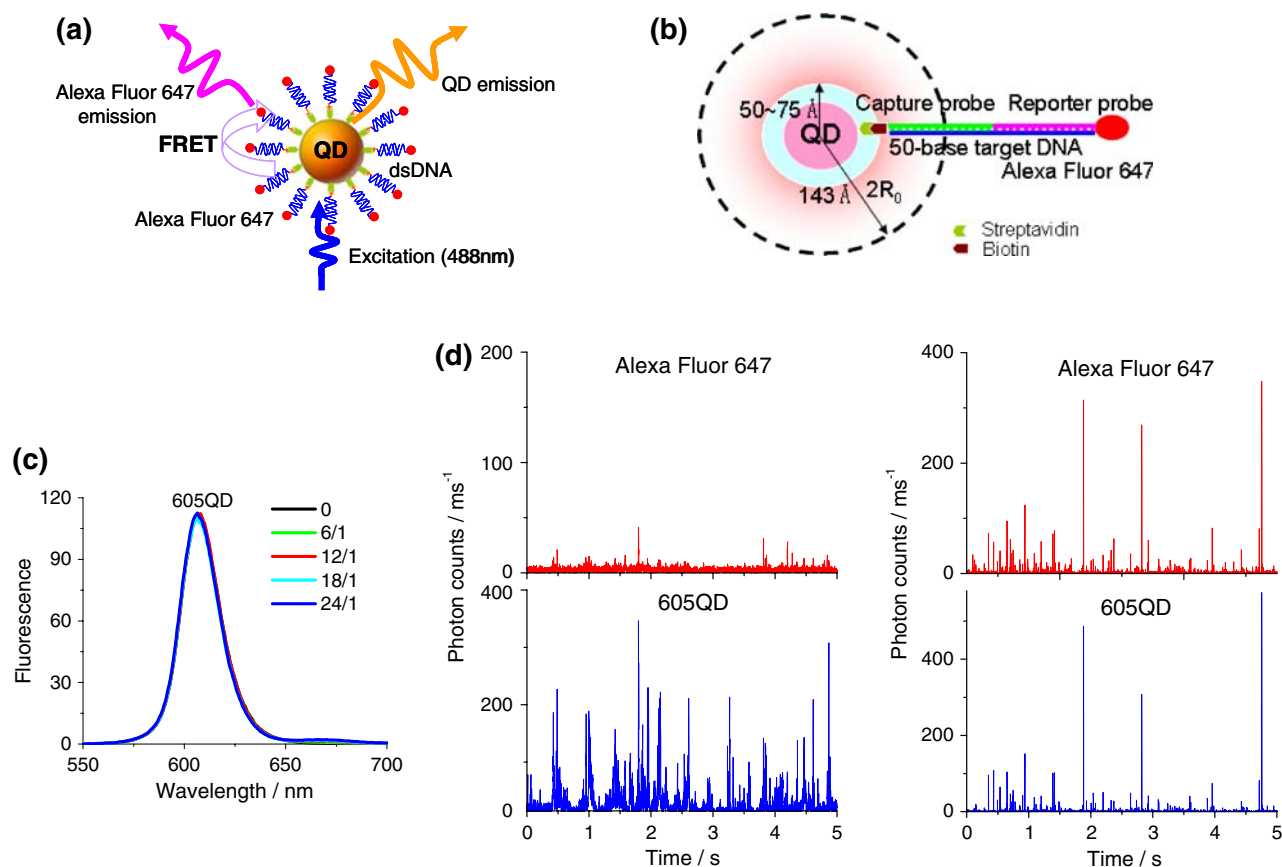
FIGURE 8. (a) Schematic depiction of the conjugate assembly using dsDNA bridge with 605-nm emitting QDs and 647 Alexa Fluor acceptor. (b) A schematic representation of the conjugate with the expected separation distance in the QD–dsDNA–Alexa Fluor 647. (c) Evolution of the ensemble fluorescence spectra as a function of the increasing DNA/QD ratio; no change was measured. (d) Representative traces of fluorescence bursts from QD–dsDNA/Alexa Fluor 647 complexes in a diffusion state (*left*, QD concentration: 0.1 nM and concentration of Alexa Fluor 647 labeled 25-mer dsDNA was 1.8 nM), and in a microfluidic flow with a flow rate of 4.0 μL/min (*right*, QD concentration = 0.02 nM and concentration of Alexa Fluor 647-labeled 25-mer dsDNA was 0.36 nM. Figure reproduced from Zhang and Johnson,[112] with permission from Wiley-VCH Verlag GmbH & Co. KGaA., and kindly provided by Dr. Zhang.

of a sandwich hybrid between the capture probe, the reporter probe, and the target sequence (as shown in Fig. 7). When mixed with SA–QDs the preformed sandwich structures bound to the QD surface, bringing several Cy5 in close proximity to the donor center in the conjugate. The solution was then introduced in a glass capillary and flowed through a small observation volume where fluorescence signals from individual bioconjugates could be detected (Fig. 7). The presence of the target was identified by the simultaneous detection of the emissions from QD (I_D) and Cy5 (I_A), indicative of the QD–DNA complex formation. This assay showed high detection sensitivity (in terms of minimal detectable target concentration) compared to molecular beacon assays employing organic dyes (Fig. 7c).

Zhang and Johnson further showed that using a similar configuration of QDs surrounded by a few hybridized oligonucleotides an increase in the flow velocity in the capillary could substantially increase the measured spFRET efficiency.[111,112] Such effect was attributed to DNA deformation in the capillary under applied Poiseuille flow field, which effectively deformed the conjugate structure and reduced the center-to-center separation distance between dye and QD. In particular, they used a 50-base target oligonucleotide sandwich-hybridized with one biotinylated 25-base capture probe and one 25-base reporter labeled with Alexa Fluor 647, similar to the configuration described above (see Fig. 8a).[112] When the sandwich hybrid oligonucleotides are immobilized on the surface of 605 nm emitting streptavidin–QDs, an average separation distance of 22–25 nm is expected from the conjugate structure together with experimental parameters under relaxed conditions (Fig. 8b). Such distance is far beyond the range of Förster
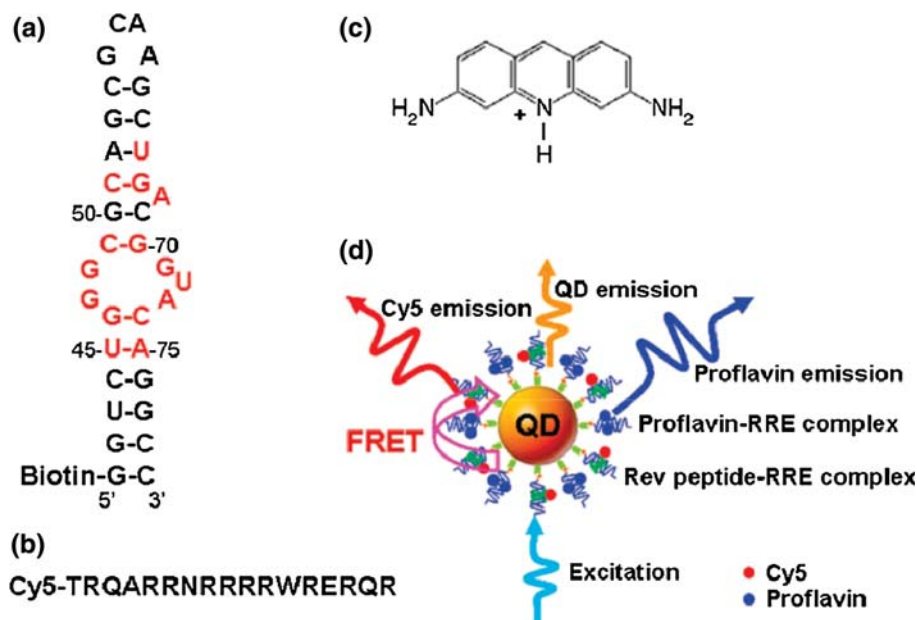
FIGURE 9. (a) Secondary structure of biotin-functionalized RRE IIB RNA. The nucleotides with strong specific affinity for Rev are highlighted in red. (b) Cy5-labeled Rev peptide used. (c) Proflavin chemical structure. (d) Schematic representation of the single-QD FRET-based sensing assembly utilized for evaluating Rev-peptide–RRE interaction along with the inhibitory efficacy of proflavin; commercial 605QD was used. Figure reproduced from Zhang and Johnson,[113] with permission from the American Chemical Society, and kindly provided by Dr. Zhang.

allowed interactions ($r > 2R_0$, R_0 being the Förster radius), and this was indeed confirmed by both sp- and ensemble FRET measurements where no QD PL quenching was measured (see Fig. 8c). However, under microfluidic flow, fluorescence bursts were clearly collected on donor and accepter channels (Fig. 8d). Furthermore, the population of events (similar to η in Fig. 5a) was found to progressively shift toward higher η (reported here as FRET efficiency) when the target concentration was increased. The latter essentially increases the number of sandwich hybrids arrayed on the nanocrystal surface, thus enhancing the FRET interactions per individual conjugate. This finding is quite interesting, as it combines the benefits of solution-phase spFRET and microfluidics to both extend the range of accessible energy transfer but also allow enhanced sensitivity to detect rather large oligonucleotides.

In a separate study Zhang and Johnson applied spFRET as a means to quantify the interactions between a specific peptide on the Rev protein (Rev-peptide) and the Rev responsive element within the RNA gene (RRE-RNA) and to identify and characterize potential inhibitors.[113] Interactions between the regulatory protein Rev and a portion of *env* gene within the RNA gene (RRE-RNA) are critical to HIV-1 replication. Rev peptide is a sequence from the basic region of Rev with reported high affinity to RRE. The authors demonstrated that the stoichiometry of

Rev-peptide binding to RRE-RNA sequence can be accurately determined using such FRET-based single QD–RRE-RNA sensing assemblies (Fig. 9). They further used this single particle configuration to potentially quantify the inhibitory effects of proflavin on the affinity between Rev-peptide and RRE. In particular, spFRET permitted them to quantify these inhibitory effects even in the presence of substantial levels of interference fluorescence from high-concentration proflavin; the latter is a blue fluorescent compound that often prevents the discrimination of FRET signals in ensemble measurements.

In all these solution phase studies, the main factors enabling efficient FRET from a QD to acceptors located at the other extremities of long double-stranded DNA and effective single molecule discrimination could be attributed to two specific features: (1) Each QD-conjugate had several sandwich hybrids arrayed around the nanocrystal surface. This increased the local acceptor concentration around the QD and resulted in high FRET efficiency as well as bright acceptor fluorescence bursts. (2) Direct excitation contribution to the acceptor signal was extremely weak, since the system could be excited in a region of minimal acceptor absorbance, which reduced the detection background to a minimal level. These two factors combined produced enhanced detection sensitivity. In the study of Zhang *et al.*,[114] for example, these QD-assemblies were successfully applied in

conjunction with an oligonucleotide ligation assay to reach single nucleotide mutation detection.

Determining the Heterogeneity of QD-Bioconjugates Using spFRET

Heterogeneity in QD-conjugates is a natural process and is due to the presence of multi-reactive sites on the surface of a QD. Thus when a surface-functionalized nanocrystal is exposed to target proteins and peptides, a distribution in the conjugate valence naturally results during the conjugate formation. We used single-QD FRET to characterize the heterogeneity of self-assembled QD-bioconjugates and to gain information about the distribution in conjugate valence.[84] These conjugates were formed by attaching (via metal-affinity driven self-assembly) average numbers of maltose binding protein (MBPs) labeled with rhodamine red (RR) onto CdSe–ZnS QDs capped with dihydrolipoic acid (DHLA) ligands. The influence of acceptor-to-donor ratio was examined by varying the fraction of labeled-to-unlabeled proteins while keeping the same total number of proteins per QD-conjugate. This study showed that within a macroscopic homogeneous sample, heterogeneity in conjugate valence is a key feature of self-assembled QD–protein conjugates. More importantly, it was shown that the number of acceptors per QD followed a Poisson distribution, where the probability of finding a conjugate having exactly n acceptors for sample with a nominal number of protein–dye per QD, N, obeys the relation[84]:

$$p(N, n) = N^n \exp(-N)/n! \qquad (1)$$

In particular, using the distribution plots shown in Fig. 5c, spFRET allowed us to determine the fraction of QD-conjugates having zero valence (i.e., QDs that are not conjugated to any MBP–dye), $p(N,0)$, for a series of macroscopic samples with increasing nominal valence, N. This was extracted from a very narrow window in the distribution of population fraction centered at $\eta = 0$ (Figs. 10a and 10b). Data clearly showed that the zero valence population fraction
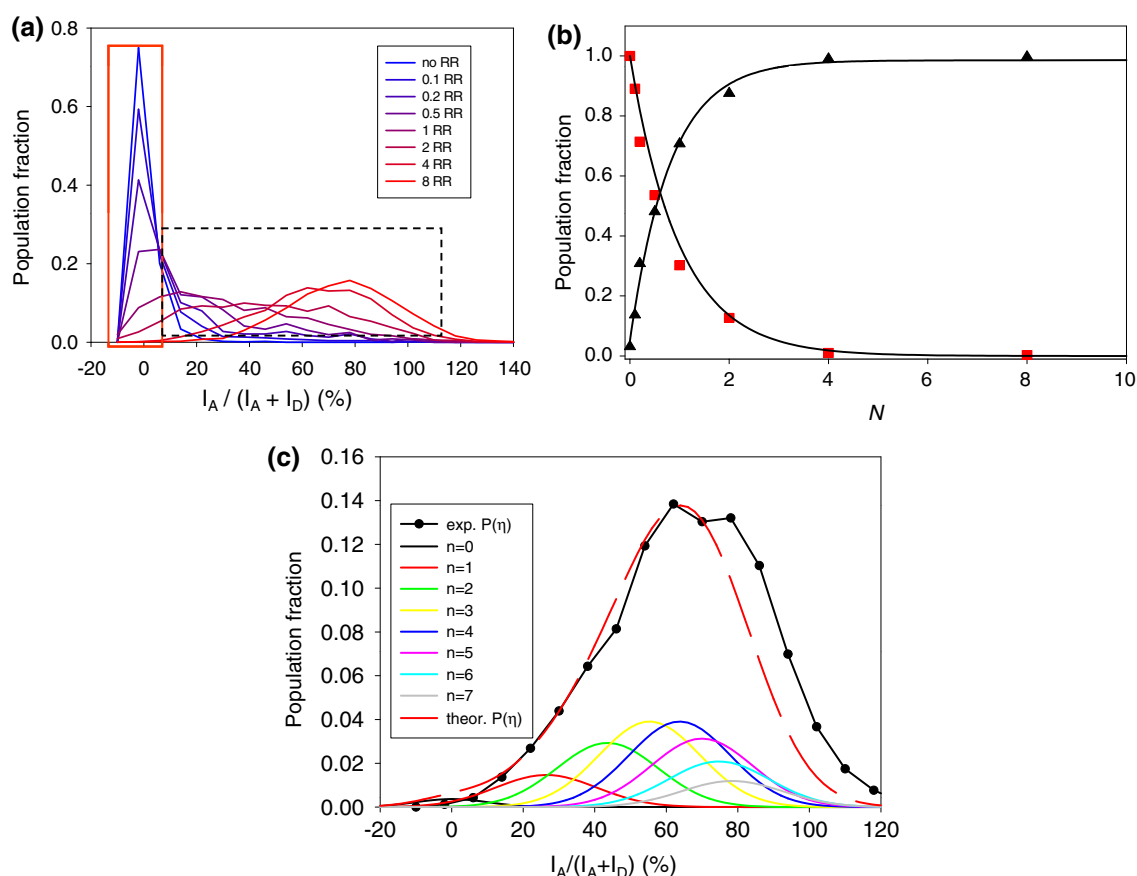

FIGURE 10. (a) spFRET population fraction vs. emission ratio η with increasing QD-conjugate valence. (b) Fraction of QDs without any acceptors or "zero valence" ($\eta < 10\%$; squares) and that engaged in FRET ($\eta > 10\%$; triangles) as a function of N, the average number of RR acceptors per QD, obtained from spFRET measurements shown in (a). The fits corresponds to the Poisson distribution $p(N,0) \sim \exp(-N)$ and $1 - p(N,0)$. (c) Comparison between predictions using Poisson function and experimental population distributions for $N = 4$. Figure partially reproduced from Pons et al.,[84] with permission from the American Chemical Society.

$(p(N,0))$ decreased exponentially with increasing N, which agrees well with the prediction of Eq. (1). The agreement between measured population distribution and the Poisson statistics was further verified for larger values of N. We used the separation distance, direct dye excitation and quantum yield ratios extracted from ensemble measurements in combination with Eq. (1) to construct a "theoretical" distribution for conjugates with exactly n dyes using Eq. (1). A composite distribution of all these sub-populations ($n = 0, 1, 2\ldots$) was then constructed using these individual distributions. A side-by-side comparison between predictions and experimental distribution for $N = 4$ is shown in Fig. 10c. There is clearly a good agreement between the Poisson distribution function and the experimental data. Additional details on applying these findings to QD–protein sensors can be found in Pons et al.[84]

IN VITRO AND IN VIVO TRACKING OF PROTEIN USING SINGLE QDS

### In Vitro Detection of Kinesin and Myosin Motor Movement

Use of single molecule tracking has elucidated the characteristics of motor proteins such as kinesin, myosin and dynein that are responsible for active intracellular transport of vesicles, organelles and protein complexes (as cargos) along microtubules or actin filaments.[42,91,98] Polymer beads of a few hundreds nanometer in size labeled (or loaded) with fluorescent dye or simply individual organic dyes were used to gain unique insights into the structural properties and movement of individual motors, determine their velocity, show that their movement is not necessarily continuous, and determine the size and rate of their steps.[42,91,98] These experiments allow observation for only a few seconds to a few tens of seconds depending on the experimental conditions, nonetheless. Use of QD tags, instead, could open up new possibilities to study the dynamic properties of these motor proteins by extending the observation times.

In this aspect, we discuss a few representative studies where use of QDs provided useful and unique information on the motion of motor proteins. In the first study, Surrey and co-worker used streptavidin–QDs to label individual biotinylated kinesin motors and track their motion characteristics with precision, including velocity, step length, and dwell time under different conditions.[92] The authors utilized QD-conjugates bearing single or multiple kinesin motors, and explored motility in configurations of crowded microtubules and in the presence of obstacles. In particular, they demonstrated that in the presence of

obstacles or in crowded conditions, kinesin motors can wait on the microtubule in a strongly bound state until the obstacle(s) unbinds, allowing the motor to move to freed site in the next step. They postulated that this behavior could explain pauses in the motion of kinesin-transported cargos observed in living cells. In another study, Warshaw et al. labeled the heads of individual myosin V motors expressing a C-terminal biotin with two different color QDs in a mixture.[102] Using two-color single QD tracking, the authors were able to locate the positions of the heads with ~6 nm precision for several minutes, follow the motion of individual myosin molecules and probe changes in their intramolecular conformation. In particular, they found that the heads on the same V motor move alternatively along the actin filament by ~74 nm steps, while maintaining an average separation distance of ~36 nm during pauses in motion. These findings confirm the predictions of the hand-over-hand model of myosin mode of motor proteins along an actin filament (Fig. 11).[108]

Conversely, QDs were used to label single fragments of the actin or microtubule, the substrate on which motors (e.g., kinesin) move. In these "sliding" assays, motors are adsorbed on a surface, and then exposed to substrate fragments. The immobilized motors are able to bind these fragments and induce their transport across the surface. A first "proof-of-principle" study by Mansson et al. demonstrated the use of QDs to label actin filaments sliding on a surface of adsorbed myosin motors, where movement of actin filaments was tracked for several seconds.[60] A more refined study published by Leduc et al. used single QDs to investigate the gliding motility of microtubules over a varying number of kinesin-1 motors attached to a glass surface. This allowed the investigation of cooperative interactions between kinesin motors with the same microtubule (MT).[52] For this, kinesin-1 motors were combined with fluorescent proteins (GFP-kinesin) then immobilized on a glass surface using 5-His antibodies, so that their locations could be determined by fluorescence imaging; additional casein allowed passivation of the rest of the surface (Fig. 12). QD-MT assemblies were then deposited on the substrate and their motion was tracked by detecting the QD emission with a ~3 nm precision (Fig. 12 bottom). By analyzing the motion, velocity and step size of microtubules interacting with one, two or higher number of kinesin-1 motors, the authors identified distinct forward and backward jumps on the order of 10 nm, which essentially indicates the existence of fractional motion steps and absence of synchronization between several motors interacting with the same microtubule. These findings led researchers to envision that the streptavidin–QDs used to label the actin filaments could also be
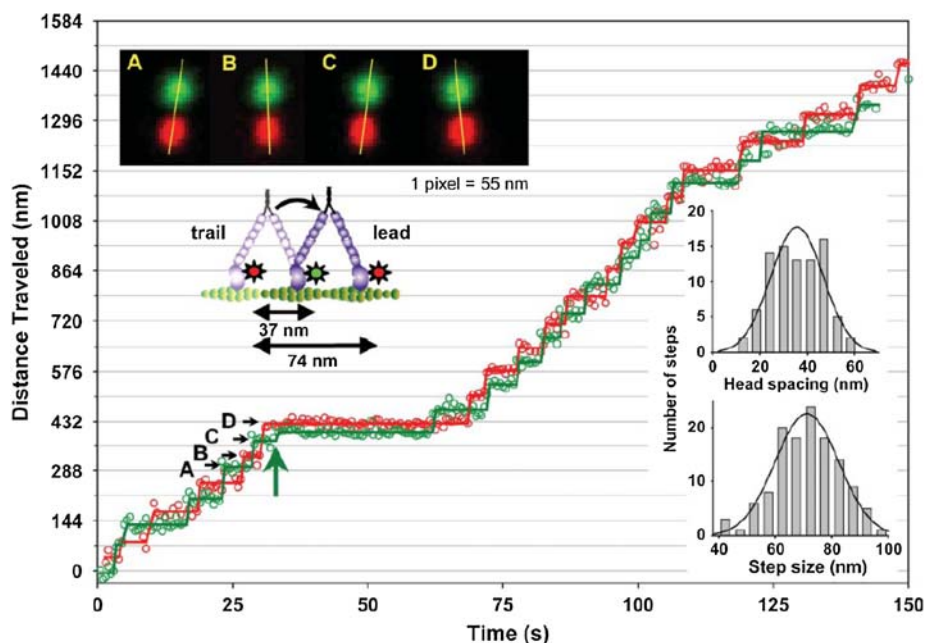
FIGURE 11.   Progressive motion of Myosin V motors labeled with red and green emitting QDs along an actin filament. Green and red open circles are the two different QD positions determined by Gaussian fits. The green arrow identifies a sub-step. Upper left are averaged QD images for steps labeled A–D. The yellow lines connect QD centers emphasizing alternating relative head positions. Histograms of inter-head spacing and step size are shown in the bottom right. Figure partially reproduced from Warshaw et al.,[102] with permission from the Biophysical Society.

used as anchor points (or a scaffold) to bind and transport large biotinylated cargos.

Tracking of Protein Receptors in Live Cells

Transposing the achievements in single QD conjugate tracking described above from *in vitro* conditions to living cells has the potential to unravel complex biomolecular interactions underlying specific cellular activities. Spatial organization of lipids, proteins, and carbohydrate on the cellular membrane plays a critical role in their interactions with the extracellular environment and surrounding tissue and in the cell signaling. Understanding when and how the cell reorganizes these membrane components is therefore a key challenge in the study of cellular activity. For instance, trafficking of neurotransmitting receptors within membrane compartments and between membrane and intracellular space plays an important role in the regulation of neuronal activity. Nonetheless, single QD tracking of receptor proteins in cell media have been successfully reported only for easily accessible targets. These include labeling of transmembrane proteins to investigate membrane-bound receptor diffusion or endosomal trafficking. Indeed, tracking of individual proteins in live cells with QDs encounters difficulties that are often shared with other nanoparticle tags and fluorophore. The main difficulty is caused by nonspecific interactions of QD-conjugates

with their environment, either due to steric hindrance (''crowding'' effects, limited access to particular cellular compartments...) or to simple non-specific adsorption of endogenous molecules on the QD surface. Other hurdles include difficulties of transfecting isolated QD-conjugates across the plasma membrane into the cytoplasm.

There has been a few promising demonstrations where some of the key properties of QDs have provided researchers the opportunity to track single transmembrane receptors for long periods of time and led to a better understanding of receptor trafficking in neurons. In a representative study, Dahan et al. reported the first use of QD for single receptor tracking in cultured neurons in 2003.[16] The authors labeled individual glycine receptors with single QD–streptavidin conjugates via primary and secondary antibodies. Single QDs were identified and tracked by their blinking properties (Fig. 13). They observed a considerably higher fluorescence signal compared to standard fluorophores, resulting in a spatial resolution reaching 5–10 nm, compared with 40 nm with an organic dye. The ability to follow the trajectory of single QD-labeled receptors for more than 20 min (compared to ~5–10 s for standard organic dyes), allowed the visualization of receptor trajectories on a time scale that was not previously accessible and revealed new diffusion dynamics. In particular, the authors showed the existence of several membrane domains corresponding
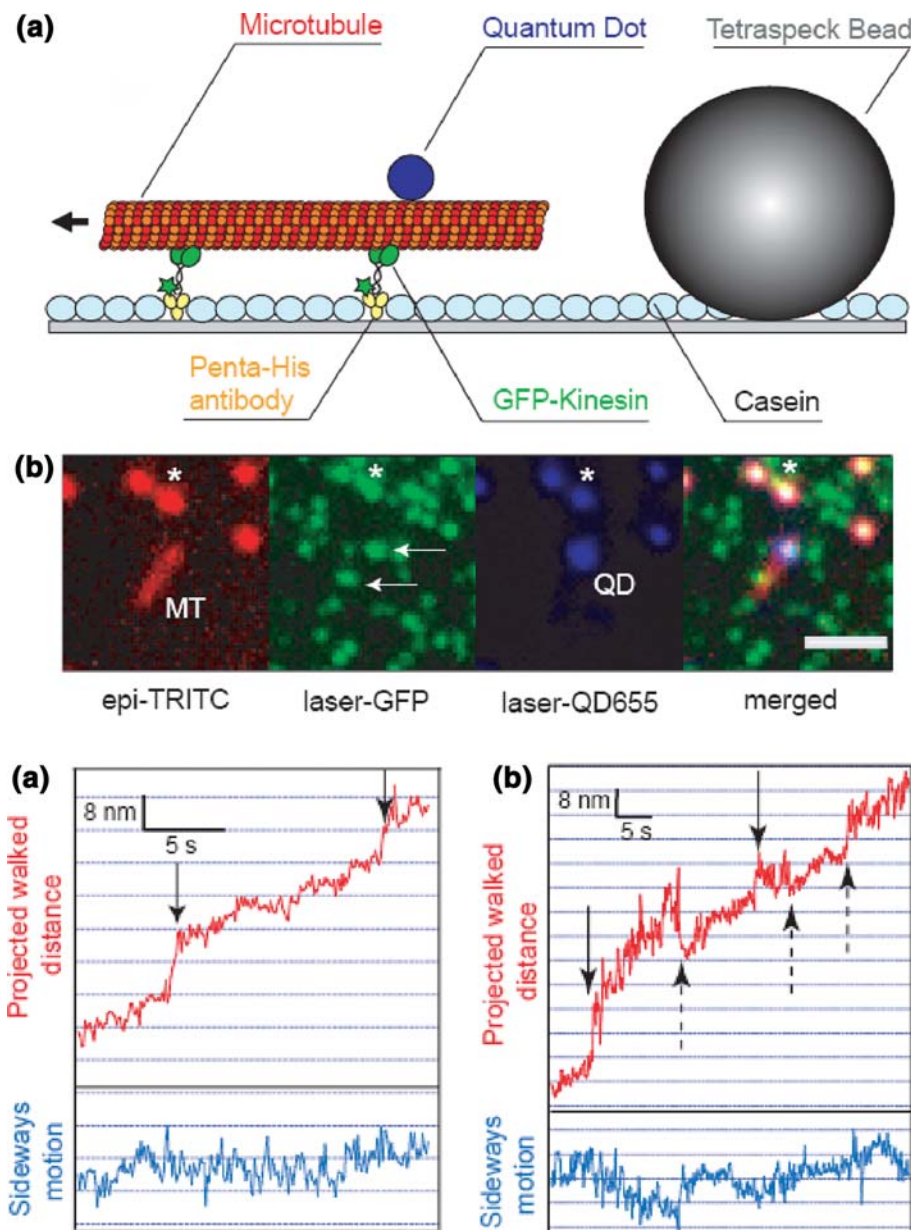
FIGURE 12. (Top) (a) Principle of an *in vitro* gliding motility assay. The fluorescent beads were used as references to correct for spatial drift. (b) Images of gliding motility, where Rhodamine-was used to visualize MTs. The positions of the GFP-kinesins (laser-GFP) and the QDs (laser-QD655) were obtained by TIRF microscopy of the same field of view. The image on the right (merged) corresponds to the overlay of the three colors. The arrowheads show the kinesin positions in the laser-GFP image. The asterisk indicates the bead position in all colors (Scale bar = 2 μm). (Bottom) Distinct jumps in the MT displacement in the three-motor case. (a and b) Projected walked distances of two QDs (red curves) and the corresponding sideways motion (blue curves). Arrows indicate the presence of jumps in the forward (solid line) and the backward (dashed line) direction. Figure partially reproduced from Leduc *et al.*,[52] with permission from the National Academy of Sciences.

to synaptic, perisynaptic and extrasynaptic regions with different receptor diffusion behaviors. A few studies have since used QDs to track trajectories of individual membrane receptors, in neurons or other cell types.[3–5,8,9,25,35,37] Single QD tracking will continue to gain more attraction in the future for studying trans-membrane protein dynamics, accessible to both specialists and non-specialists.

Recently, Tsien and co-workers used fluctuations in single QD intensities as a means to probe of their chemical environment, in addition to their localization.[115] The authors were able to measure relevant neuro-physiological parameters that were previously inaccessible, such as kiss-and-run and full-collapse fusion intervals and occurrences, fusion pore open time and kinetics of re-acidification of the vesicle
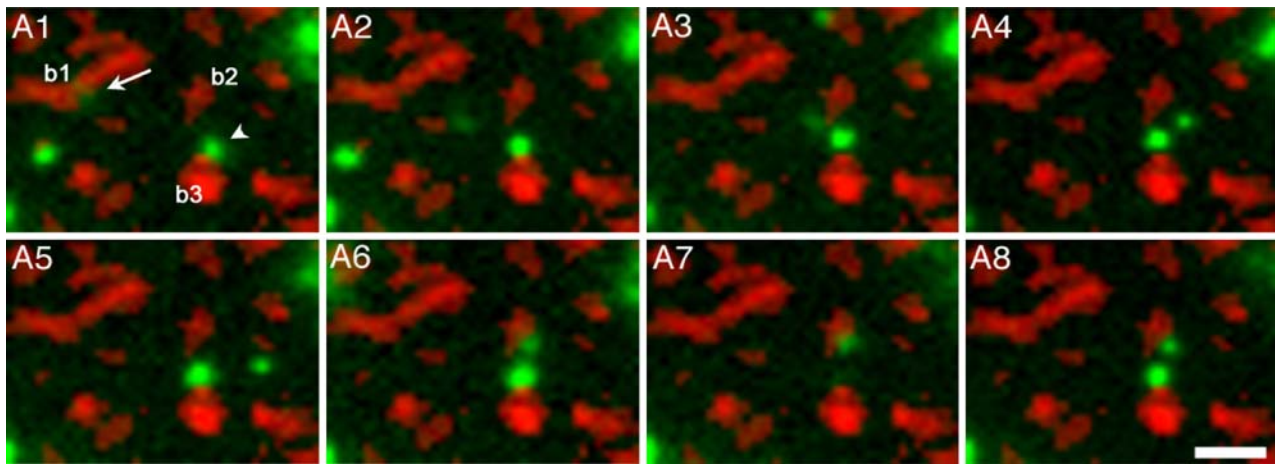
FIGURE 13. Visualization of multiple exchanges between extrasynaptic and synaptic domains, in which an individual Glycene receptor (GlyR) alternated between free and confined diffusion states. Images extracted from a sequence of 850 frames (acquisition time: 75 ms). (A1) to (A8) correspond to frames 6, 118, 150, 267, 333, 515, 629, and 850, respectively. QD fluorescence spots (green) and FM4-64-labeled synaptic boutons (red). One QD (arrow), first located at bouton b1, diffuses in the extrasynaptic membrane [(A2) to (A5)] and associates with bouton b2 [(A6) to (A8)]. Scale bar, 2 μm. Figure reproduced from Dahan et al.,[16] with permission from AAS.
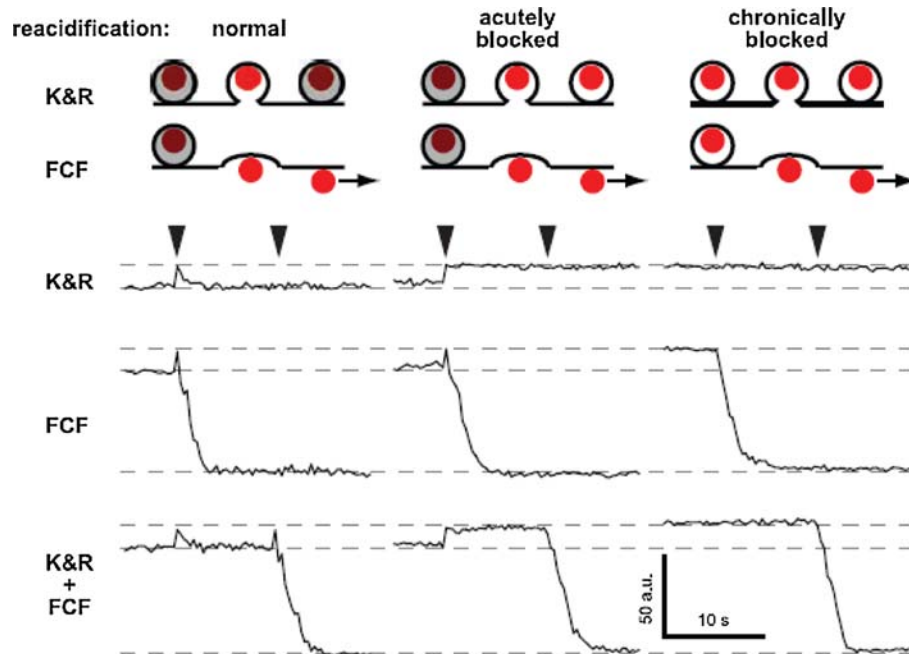

FIGURE 14. Experimental traces illustrating typical emission patterns under three conditions, which are classified as K&R, FCF, or K&R + FCF. Also shown is a schematic depiction of the hypothesized effect of acute or chronic block of vesicular H+-adenosine triphosphatase with bafilomycin A1 (Baf). Without Baf (normal), QD emission is reduced (maroon) by acidic luminal pH (gray). Vesicle fusion deacidifies the environment producing QD brightening (red). Acute application of Baf (acutely blocked) prevents reacidification after vesicle retrieval; chronic Baf (chronically blocked) removes all pH gradients. Figure reproduced from Zhang et al.,[115] with permission from AAAS.

interior. They incubated hippocampal neurons with QDs so that they can be loaded into intracellular vesicles at synapses. Electrical stimulation of the neurons elicited vesicle exocytosis, which occurred following either "full-collapse fusion" (FCF) or "kiss-and-run" (K&R). Whereas in FCF, the vesicle fully fuses with

the cell membrane and loses its identity, in K&R the vesicle fuses transiently with the cell membrane to release its content into the extracellular medium through a 1–5 nm pore and is then rapidly recycled/reformed (see Fig. 14). FCF of a QD-containing vesicle is easily detected by diffusion of the QD out of the vesicle into
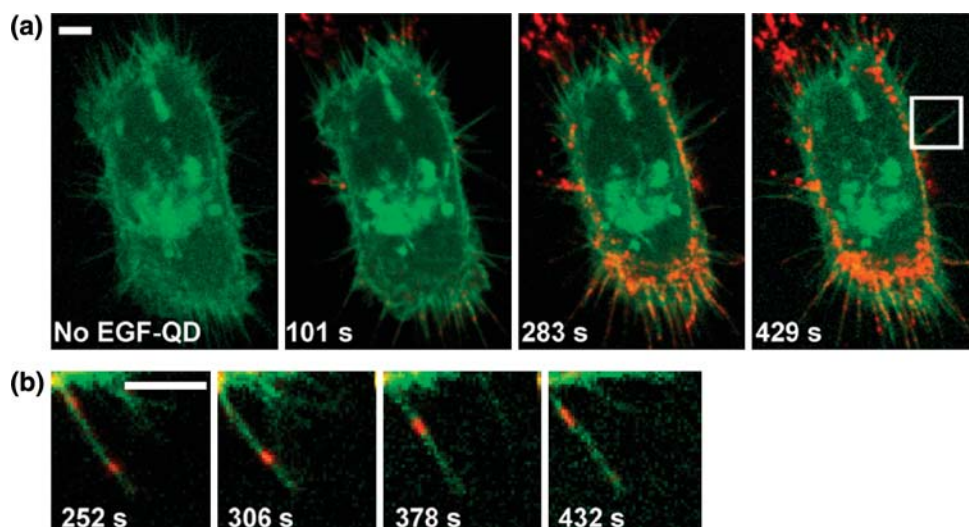
FIGURE 15. Retrograde transport of EGF-QDs (red) on filipodia. (a) A431 cell expressing receptor erbB3-mCitrine (green); maximum intensity projection of four 0.5 μm confocal sections as a function of time. (b) Magnified image of filipodium indicated in the last panel of (a), showing the uniform migration of the EGF–QDs toward the cell body with a velocity of ~10 nm/s. All scale bars, 5 μm. Figures reproduced from Lidke et al.,[56] with permission from the Nature Publishing Group.

the extracellular medium. In comparison, during K&R, the QD stays inside the vesicle. The internal pH of normal vesicles is ~5.5, but during K&R, this pH is equilibrated (through the fusion pore) with that of the external medium, and increases to ~7. When the pore closes and the vesicle recovers its integrity, its internal medium is re-acidified to pH 5.5. To detect K&R events, the authors relied on the pH-dependence of QD PL (~15% change in ensemble PL between pH 5.5 and pH 7.4). This pH change translated into a ~15% increase single QD PL while the fusion pore was open, and a decrease back to its initial level when the vesicle recovers its initial pH. The exact mechanism responsible for the pH dependence of the QD PL was not elucidated, however. In addition, measuring reproducible small changes in single QD PL due to small pH changes is still an open question; the authors showed homogeneous single QD emission with rather low signal noise levels beyond what has often been reported in the literature. Issues related to reproducibility and stability of hydrophilic QDs we discussed previously were simply not been discussed in this report. Future studies will require control over (and understanding of) the QD sensitivity to pH changes in order to obtain reproducible, specific QD PL responses to different chemical environments. The results reported by Zhang et al.,[115] nonetheless, constitute a step forward in using single QD spectroscopy.

QDs have also given access to new information regarding endosomal trafficking of trans-membrane receptors. A study by Lidke et al. in 2004 demonstrated that QDs conjugated to the epidermal growth factor (EGF) using streptavidin–biotin binding could be used to monitor the binding of EGF to specific membrane receptors and track their intracellular fate (Fig. 15).[56] EGF–QDs were shown to correctly bind and activate the targeted erbB1 receptor, followed by endocytotic uptake of the EGF–QD–receptor complex. The authors were then able to track the trajectories of individual EGF–QD–receptor and show the existence of a new retrograde transport mechanism in filopodia from the cell surface to the cell body. In a subsequent study, the authors used single EGF–QD tracking to examine the nature of this retrograde transport in detail.[55] In particular, analysis of single QD trajectories and their mean square displacements showed a behavior consistent with active transport and not a Brownian motion. The authors showed that this transport was supported by the actin network, as indicated by analysis of transport velocities and the effects of pharmacological agents. They next exposed the cells to two different colors of EGF–QD conjugates and observed that the onset of active transport correlated with merging of two EGF–QD conjugates. This showed that dimerization of EGF-activated receptors was necessary to trigger the active transport. Finally, they examined whether retrograde transport occurred before or after endocytosis of the EGF–QD–receptor conjugates using FRET between QD donors and organic dyes. Membrane-impermeable biotinylated dyes were able to bind the remaining biotin-binding sites on QD–EGF conjugates, resulting in efficient FRET, even after the onset of retrograde transport. This demonstrated that these conjugates were still available to the

extracellular medium, and that receptor endocytosis only occurred after retrograde transport along the filopodia, when reaching the cell body. In another study, Vu and co-worker used antibody-conjugated QDs to target specific membrane receptors to the nerve growth factor.[88] The authors showed that QDs allowed monitoring not only of the receptor cellular uptake, but also of its intracellular fate. QD-labeled receptor processing by the cells was consistent with that of unlabeled receptors, including active shuttling of QD–receptors conjugates to new neural processes.

In a different study, Weiss and co-workers used the process of avidin polypeptide chain fusion to the glycosylphosphatidylinositol (GPI)–anchoring sequence of human CD14 receptors as a means to target avidin receptors expressed in the cytoplasmic membrane of HeLa cells. For this they used the direct peptide cap exchange approach on the QDs they recently developed and employed biotin-peptide-coated CdSe–ZnS QDs to label the avidin receptors expressed in the cytoplasmic membrane of these HeLa cells, and followed their motion using single molecule resolution. They in particular tracked the bound QD–peptide conjugates for several minutes as they diffused in the membrane of live cells and trafficked in the cytosol.[69,82] This allowed them to probe the relationship between GPI-anchored receptors and lipid rafts in the cell membrane.

Using the same peptide surface coating strategy Weiss and co-workers further developed a general platform to use QDs for labeling and tracking of cell membrane proteins at the single molecule level. They started by inserting a small fraction of hapten-modified peptides (along with PEG-appended peptide) during the hydrophilic transfer of their QDs, producing hapten-functionalized nanocrystals with reduced non-specific interactions. The haptens were then used to target cell surface fusion protein containing single chain antibody fragments (scFVs) specific to haptens. In this design, a scFV and the corresponding hapten recognition pair are separately attached to the target protein and the QD, respectively. They then applied this strategy to probe the specific affinity between 4M5.3 scFv developed against fluorescein. In particular they demonstrated targeting of 4M5.3 scFv displayed on the membrane of yeast and murine neuronal cells.[44] Figure 16 shows a test of these probes on a mobile target protein mouse prion protein (PrP) expressed on
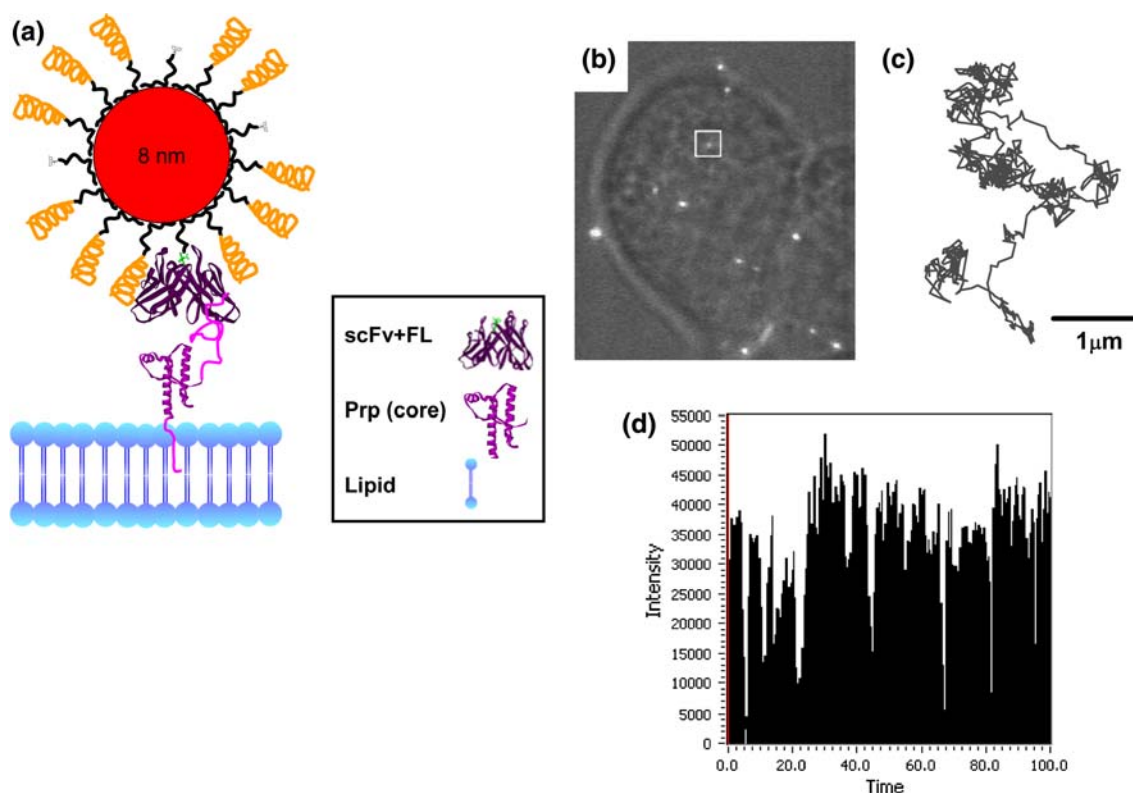
FIGURE 16. (a) Cartoon representation of a scFv–PrP anchored in the membrane of an N2a cell via its GPI-anchor with a bound fluorescein-peptide-coated QD (FL-pc-QD). (b–d) Single-particle tracking of scFv–PrP in live neuroblastoma cells immobilized on a glass coverslip. (b) DIC image with overlaid QD fluorescence (white spots). (c) Thousand frames single-QD trajectory of the QD indicated by the white square in (b). (d) Intensity time trace exhibiting a blinking pattern typical of a single QD. Scale bars are 10 μm in (b) and 1 μm in (c). Figure partially reproduced from Iyer et al.,[44] with permission from the American Chemical Society.

neuroblastoma cell line N2a, where the scFv was fused to the N-terminus of PrP. The trajectory isolated for a single QD–hapten conjugate indicates that there are two distinct diffusion regimes for the protein on the immobilized cell membrane; single protein movement was identified by the intermittent (blinking) fluorescence signal typical of individual QD emission.

In order to circumvent some of the limitations associated with effective uptake of QD-bioconjugates across the cell membrane, Courty and co-workers used osmotic lysis of pinosomes to deliver individual QD–kinesin-motor conjugates inside the cell cytoplasm.[22] This mode of delivery involves exposure of the cells to first a hyper-osmotic solution to induce QD pinocytosis, then to a hypo-osmotic solution to disrupt the pinosomes and release their content. The authors reported that conjugates delivered via this mechanism could be tracked individually over time. They found that the majority of QD-conjugates showed trajectories typical of freely diffusing Brownian motion, but a smaller fraction (~10%) of conjugates exhibited a rather linear directed motion. This directed motion was not observed when using unconjugated QDs or when inhibiting kinesin motor transport by a chemically induced depolymerization of the actin filaments. When analyzing the directed motion of this fraction of QD-conjugates, the authors observed a velocity consistent *with in vitro* observations, which show that kinesin movement was not affected by its QD cargo. This study is particularly encouraging for future developments using QDs to track individual biomolecules in the cytoplasm. Nonetheless, additional systematic studies using a variety of cell types will still be needed to validate this type of cellular delivery and to ensure the absence of non-specific interactions of the QDs with the complex intracellular environment.

The few studies described in this report clearly indicate that QDs have the potential to offer valuable insights into intracellular trafficking of membrane receptors and can reveal previously inaccessible transport mechanisms. The studies exploited the high photo-resistance of QDs to track individual emitters for long period of time and report the trafficking of the conjugated biomolecules. In general, the main limitations of these techniques originate from the still relatively large size of the QD conjugates, which may influence the QD-labeled protein diffusion in confined spaces like synaptic clefts, or from non-specific interactions with endogenous molecules. The size limitation adds constraints even to probing extracellular transmembrane protein tracking (e.g., due to the presence of large transmembrane carbohydrates). Blinking of QD fluorescence though often causes occasional interruption of the reconstructed trajectories, has not seriously

limited the use of QDs in single protein tracking as long as the density of labeled receptors is low enough that the same QD can be identified again during the next emitting period. Blinking has indeed been used as means to distinguish single QD-conjugate from those of aggregates, and it has allowed unequivocal identification and tracking of single molecules in macroscopic samples. However, it may be necessary to correct quantitative transport measurements from QD blinking effect in certain applications.[22]

CONCLUSION

By allowing measurements with high signal-to-noise ratios and extended observation times, QDs have clearly opened up new possibilities for studying a variety of biological processes at the single molecule level. For example, they allowed tracking of single protein receptor trajectories with high spatial resolution and over several tens of minutes. The set of single molecule studies summarized in this review constitute only a small fraction of what use of QD fluorophores promises in biology. In addition to improving existing single biomolecule assays these materials have the potential to allow access to previously inaccessible information about biomolecular interactions, as has been demonstrated in a few preliminary *in vitro* and live cell studies. One should expect that optical techniques for single molecule tracking, in particular, will tremendously benefit from further development in QD functionalization and conjugation techniques. Further progress combined with extended observation times will bring even better spatial and temporal resolution of reconstructed trajectories inside live cells.

However, further progress in several domains will be required in order to take advantage of the full potential of these materials and realize the potentials of single QDs studies. In particular, better and sound characterization of the effects of surface coating and conjugation strategies on the long-term stability of QDs and QD-bioconjugates in buffers and in intracellular environments is needed. Intracellular compartments are complex and usually rich in ionic materials, and non-specific interactions often alter QD movements in these media. One can expect that as better and more controllable surface functionalization strategies are developed and improved QD stability in biological media and easy to implement conjugation strategies become available, single molecule assays using QDs will ultimately transition from proof-of-principles performed by specialists to general use by the broader biological and biophysical community.

ACKNOWLEDGMENTS

REFERENCES

[1]Agrawal, A., C. Y. Zhang, T. Byassee, R. A. Tripp, and S. Nie. Counting single native biomolecules and intact viruses with color-coded nanoparticles. *Anal. Chem.* 78:1061–1070, 2006. doi:10.1021/ac051801t.

[2]Anikeeva, N., T. Lebedeva, A. R. Clapp, E. R. Goldman, M. L. Dustin, H. Mattoussi, and Y. Sykulev. Quantum dot–peptide-MHC biosensors reveal strong CD_8-dependent cooperation between self and viral antigens that augment the T cell response. *Proc. Natl. Acad. Sci.* 103:16846–16851, 2006. doi:10.1073/pnas.0607771103.

[3]Bats, C., L. Groc, and D. Choquet. The interaction between stargazin and PSD-95 regulates AMPA receptor surface trafficking. *Neuron* 53:719–734, 2007. doi:10.1016/j.neuron.2007.01.030.

[4]Bouzigues, C., and M. Dahan. Transient directed motions of GABA(A) receptors in growth cones detected by a speed correlation index. *Biophys. J.* 92:654–660, 2007. doi:10.1529/biophysj.106.094524.

[5]Bouzigues, C., M. Morel, A. Triller, *et al.* Asymmetric redistribution of GABA receptors during GABA gradient sensing by nerve growth cones analyzed by single quantum dot imaging. *Proceed. Nat. Acad. Sci.* 104:11251–11256, 2007. doi:10.1073/pnas.0702536104.

[6]Bruchez, M., Jr., M. Moronne, P. Gin, S. Weiss, and A. P. Alivisatos. Semiconductor nanocrystals as fluorescent biological labels. *Science* 281:2013–2016, 1998. doi:10.1126/science.281.5385.2013.

[7]Carion, O., B. Mahler, T. Pons, and B. Dubertret. Synthesis, encapsulation, purification and coupling of single quantum dots in phospholipid micelles for their use in cellular and in vivo imaging. *Nat. Protocols* 2:2383–2390, 2007. doi:10.1038/nprot.2007.351.

[8]Charrier, C., M. V. Ehrensperger, M. Dahan, *et al.* Cytoskeleton regulation of glycine receptor number at synapses and diffusion in the plasma membrane. *J. Neurosci.* 26:8502–8511, 2006. doi:10.1523/JNEUROSCI.1758-06.2006.

[9]Chen, H. F., I. Titushkin, M. Stroscio, *et al.* Altered membrane dynamics of quantum dot-conjugated integrins during osteogenic differentiation of human bone marrow derived progenitor cells. *Biophys. J.* 92:1399–1408, 2007. doi:10.1529/biophysj.106.094896.

[10]Chen, Y. F., J. Vela, H. Htoon, J. L. Casson, D. J. Werder, D. A. Bussian, V. I. Klimov, and J. A. Hollingsworth. "Giant" multishell CdSe nanocrystal quantum dots with suppressed blinking. *J. Am. Chem. Soc.* 130:5026–5027, 2008. doi:10.1021/ja711379k.

[11]Clapp, A. R., I. L. Medintz, and H. Mattoussi. Förster resonance energy transfer investigations using quantum-dot fluorophores. *ChemPhysChem* 7:47–57, 2006. doi:10.1002/cphc.200500217.

[12]Clapp, A. R., I. L. Medintz, J. M. Mauro, B. R. Fisher, M. G. Bawendi, and H. Mattoussi. Fluorescence resonance energy transfer between quantum dot donors and dye-labeled protein acceptors. *J. Am. Chem. Soc.* 126:301–310, 2004. doi:10.1021/ja037088b.

[13]Coe, S., W.-K. Woo, M. Bawendi, and V. Bulovic. Electroluminescence from single monolayers of nanocrystals in molecular organic devices. *Nature* 420:800–803, 2002. doi:10.1038/nature01217.

[14]Crut, A., B. Geron-Landre, I. Bonnet, S. Bonneau, P. Desbiolles, and C. Escude. Detection of single DNA molecules by multicolor quantum-dot end-labeling. *Nucleic Acids Res.* 33:e98, 2005. doi:10.1093/nar/gni097.

[15]Dabbousi, B. O., J. Rodriguez-Viejo, F. V. Mikulec, J. R. Heine, H. Mattoussi, R. Ober, K. F. Jensen, and M. G. Bawendi. (CdSe)ZnS core–shell quantum dots: synthesis and characterization of a size series of highly luminescent nanocrystallites. *J. Phys. Chem. B* 101:9463–9475, 1997. doi:10.1021/jp971091y.

[16]Dahan, M., S. Levi, C. Luccardini, P. Rostaing, B. Riveau, and A. Triller. Diffusion dynamics of glycine receptors revealed by single-quantum dot tracking. *Science* 302:442–445, 2003. doi:10.1126/science.1088525.

[17]Deniz, A. A., M. Dahan, J. R. Grunwell, *et al.* Single-pair fluorescence resonance energy transfer on freely diffusing molecules: Observation of Förster distance dependence and subpopulations. *Proc. Natl. Acad. Sci.* 96:3670–3675, 1999. doi:10.1073/pnas.96.7.3670.

[18]Deniz, A. A., T. A. Laurence, M. Dahan, *et al.* Ratiometric single-molecule studies of freely diffusing biomolecules. *Ann. Rev. Phys. Chem.* 52:233–253, 2001. doi:10.1146/annurev.physchem.52.1.233.

[19]Du, H., C. Chen, R. Krishnan, T. D. Krauss, J. M. Harbold, F. W. Wise, M. G. Thomas, and J. Silcox. Optical properties of colloidal PbSe nanocrystals. *Nano Lett.* 2:1321–1324, 2002. doi:10.1021/nl025785g.

[20]Duan, H., and S. Nie. Cell-penetrating quantum dots based on multivalent and endosome-disrupting surface coatings. *J. Am. Chem. Soc.* 129:3333–3338, 2007. doi:10.1021/ja068158s.

[21]Dubertret, B., P. Skourides, D. J. Norris, V. Noireaux, A. H. Brivanlou, and A. Libchaber. In vivo imaging of quantum dots encapsulated in phospholipid micelles. *Science* 298:1759–1762, 2002. doi:10.1126/science.1077194.

[22]Durisic, N., A. I. Bachir, D. L. Kolin, *et al.* Detection and correction of blinking bias in image correlation transport measurements of quantum dot tagged macromolecules. *Biophys. J.* 93:1338–1346, 2007. doi:10.1529/biophysj.107.106864.

[23]Edgar, R., M. McKinstry, J. Hwang, *et al.* High-sensitivity bacterial detection using biotin-tagged phage and quantum-dot nanocomplexes. *Proc. Natl. Acad. Sci.* 103:4841–4845, 2006. doi:10.1073/pnas.0601211103.

[24]Efros, Al. L., and M. Rosen. Random telegraph signal in the photoluminescence intensity of a single quantum dot. *Phys. Rev. Lett.* 78:1110–1113, 1996.

[25]Ehrensperger, M. V., C. Hanus, C. Vannier, *et al.* Multiple association states between glycine receptors and gephyrin identified by SPT analysis. *Biophys. J.* 92:3706–3718, 2007. doi:10.1529/biophysj.106.095596.

[26]Empedocles, S. A., D. J. Norris, and M. G. Bawendi. Photoluminescence spectroscopy of single CdSe nanocrystallite quantum dots. *Phys. Rev. Lett.* 77:3873, 1996. doi:10.1103/PhysRevLett.77.3873.

[27]Fan, H., E. W. Leve, C. Scullin, J. Gabaldon, D. Tallant, S. Bunge, T. Boyle, M. C. Wilson, and C. J. Brinker. Surfactant-assisted synthesis of water-soluble and biocompatible semiconductor quantum dot micelles. *Nano Lett.* 5:645–648, 2005. doi:10.1021/nl050017l.

[28]Gao, X. H., Y. Y. Cui, R. M. Levenson, L. W. K. Chung, and S. M. Nie. In vivo cancer targeting and imaging with semiconductor quantum dots. *Nat. Biotechnol.* 22:969–976, 2004. doi:10.1038/nbt994.

[29]Gaponenko, S. V. Optical Properties of Semiconductor Nanocrystals, Vol. 23. Cambridge: Cambridge University Press, 1998.

[30]Gerion, D., F. Pinaud, S. C. Williams, W. J. Parak, D. Zanchet, S. Weiss, and A. P. Alivisatos. Synthesis and properties of biocompatible water-soluble silica-coated CdSe/ZnS semiconductor quantum dots. *J. Phys. Chem. B* 105:8861–8871, 2001. doi:10.1021/jp0105488.

[31]Goldman, E. R., A. R. Clapp, G. P. Anderson, H. T. Uyeda, J. M. Mauro, I. L. Medintz, and H. Mattoussi. Multiplexed toxin analysis using four colors of quantum dot fluoro-reagents. *Anal. Chem.* 76:684–688, 2004. doi:10.1021/ac035083r.

[32]Greenham, N. C., X. G. Peng, and A. P. Alivisatos. Charge separation and transport in conjugated-polymer/semiconductor-nanocrystal composites studied by photoluminescence quenching and photoconductivity. *Phys. Rev. B* 54:17628, 1996. doi:10.1103/PhysRevB.54.17628.

[33]Guo, W., J. Li, Y. A. Wang, and X. Peng. Conjugation chemistry and bio-applications of semiconductor box-nanocrystals prepared via dendrimer-bridging. *Chem. Mater.* 15:3125–3133, 2003. doi:10.1021/cm034341y.

[34]Ha, T., T. Enderle, D. F. Ogletree, *et al.* Probing the interaction between two single molecules: fluorescence resonance energy transfer between a single donor and a single acceptor. *Proc. Natl. Acad. Sci.* 93:6264–6268, 1996. doi:10.1073/pnas.93.13.6264.

[35]Haggie, P. M., J. K. Kim, G. L. Lukacs, *et al.* Tracking of quantum dot-labeled CFTR shows near immobilization by C-terminal PDZ interactions. *Mol. Biol. Cell* 17:4937–4945, 2006. doi:10.1091/mbc.E06-08-0670.

[36]Hahn, M. A., J. S. Tabb, and T. D. Krauss. Detection of single bacterial pathogens with semiconductor quantum dots. *Anal. Chem.* 77:4861–4869, 2005. doi:10.1021/ac050641i.

[37]Heine, M., L. Groc, R. Frischknecht, J.-C. Béïque, B. Lounis, G. Rumbaugh, R. L. Huganir, L. Cognet, and D. Choquet. Surface mobility of postsynaptic AMPARs tunes synaptic transmission. *Science* 320:201–205, 2008. doi:10.1126/science.1152089.

[38]Henglein, A. Photodegradation and fluorescence of colloidal cadmium sulfide in aqueous solution. *Ber. Bunsen-Ges. Phys. Chem.* 86:301–305, 1982.

[39]Hines, M. A., and P. Guyot-Sionnest. Synthesis and characterization of strongly luminescing ZnS-capped CdSe nanocrystals. *J. Phys. Chem.* 100:468–471, 1996.

[40]Ho, Y. P., M. C. Kung, S. Yang, *et al.* Multiplexed hybridization detection with multicolor colocalization of quantum dot nanoprobes. *Nano Lett.* 5:1693–1697, 2005. doi:10.1021/nl050888v.

[41]Hohng, S., and T. Ha. Single-molecule quantum-dot fluorescence resonance energy transfer. *ChemPhysChem* 6:956–960, 2005. doi:10.1002/cphc.200400557.

[42]Hurtley, S. M., and L. Helmuth (Eds.). Special issue on biological imaging. *Science* 300, 2003.

[43]Huynh, W. U., J. J. Dittmer, and A. P. Alivisatos. Hybrid nanorod-polymer solar cells. *Science* 295:2425–2427, 2002. doi:10.1126/science.1069156.

[44]Iyer, G., X. Michalet, Y.-P. Chang, F. F. Pinaud, S. E. Matyas, G. Payne, and S. Weiss. High affinity scFv hapten pair as a tool for quantum dot labeling and tracking of single proteins in live cells. *Nano Lett.* 8:4618–4623, 2008.

[45]Jaiswal, J. K., H. Mattoussi, J. M. Mauro, *et al.* Long-term multiple color imaging of live cells using quantum dot bioconjugates. *Nat. Biotechnol.* 21:47–51, 2003. doi:10.1038/nbt767.

[46]Kim, S., Y. T. Lim, E. G. Soltesz, A. M. De Grand, J. Lee, A. Nakayama, J. A. Parker, T. Mihaljevic, R. G. Laurence, D. M. Dor, L. H. Cohn, M. G. Bawendi, and J. V. Frangioni. Near-infrared fluorescent type II quantum dots for sentinel lymph node mapping. *Nat. Biotechnol.* 22:93–97, 2004. doi:10.1038/nbt920.

[47]Kippeny, T., L. A. Swafford, and S. J. Rosenthal. Semiconductor nanocrystals: a powerful visual aid for introducing the particle in a box. *J. Chem. Educ.* 79:1094–1100, 2002.

[48]Kortan, A. R., R. Hull, R. L. Opila, M. G. Bawendi, M. L. Steigerwald, P. J. Carrolla, and L. E. Brus. Nucleation and growth of CdSe on ZnS quantum crystallite seeds, and vice versa, in inverse micelle media. *J. Am. Chem. Soc.* 112:1327–1332, 1990. doi:10.1021/ja00160a005.

[49]Kuno, M., D. P. Fromm, H. F. Hamann, A. Gallagher, and D. J. Nesbitt. "On"/"off" fluorescence intermittency of single semiconductor quantum dots. *J. Chem. Phys.* 115:1028–1040, 2001. doi:10.1063/1.1377883.

[50]Kuno, M., D. P. Fromm, S. T. Johnson, A. Gallagher, and D. J. Nesbitt. Modeling distributed kinetics in isolated semiconductor quantum dots. *Phys. Rev. B* 67:125304, 2003. doi:10.1103/PhysRevB.67.125304.

[51]Larson, D. R., W. R. Zipfel, R. M. Williams, S. W. Clark, M. P. Bruchez, F. W. Wise, and W. W. Webb. Water-soluble quantum dots for multiphoton fluorescence imaging in vivo. *Science* 300:1434–1436, 2003. doi:10.1126/science.1083780.

[52]Leduc, C., F. Ruhnow, J. Howard, and S. Diez. Detection of fractional steps in cargo movement by the collective operation of kinesin-1 motors. *Proc. Natl. Acad. Sci.* 104:10847–10852, 2007. doi:10.1073/pnas.0701864104.

[53]Levy, M., S. F. Cater, and A. D. Ellington. Quantum-dot aptamer beacons for the detection of proteins. *ChemBioChem* 6:2163–2166, 2005. doi:10.1002/cbic.200500218.

[54]Li, J. J., Y. A. Wang, W. Guo, J. C. Keay, T. D. Mishima, M. B. Johnson, and X. Peng. Large-scale synthesis of nearly monodisperse CdSe/CdS core/shell nanocrystals using air-stable reagents via successive ion layer adsorption and reaction. *J. Am. Chem. Soc.* 125:12567–12575, 2003. doi:10.1021/ja0363563.

[55]Lidke, D. S., K. A. Lidke, B. Rieger, T. M. Jovin, and D. Arndt-Jovin. Reaching out for signals: filopodia sense EGF and respond by directed retrograde transport of activated receptors. *J. Cell Biol.* 170:619–626, 2005. doi:10.1083/jcb.200503140.

[56]Lidke, D. S., P. Nagy, R. Heintzmann, D. J. Arndt-Jovin, J. N. Post, H. E. Grecco, E. A. Jares-Erijman, and T. M. Jovin. Quantum dot ligands provide new insights into erbB/HER receptor-mediated signal transduction. *Nat. Biotechnol.* 22:198–203, 2004. doi:10.1038/nbt929.

[57]Lin, C. A. J., R. A. Sperling, J. K. Li, T. Y. Yang, P. Y. Li, M. Zanella, W. H. Chang, and W. G. Parak. Design of an amphiphilic polymer for nanoparticle coating and

functionalization. *Small* 4:334–341, 2008. doi:10.1002/smll.200700654.

58Liu, W., M. Howarth, A. B. Greytak, Y. Zheng, D. G. Nocera, A. Y. Ting, and M. G. Bawendi. Compact biocompatible quantum dots functionalized for cellular imaging. *J. Am. Chem. Soc.* 130:1274–1284, 2008. doi:10.1021/ja076069p.

59Mahler, B., P. Spinicelli, S. Buil, X. Quelin, J.-P. Hermier, and B. Dubertret. Towards non-blinking colloidal quantum dots. *Nat. Mater.* 7:659–664, 2008. doi:10.1038/nmat2222.

60Mansson, A., M. Sundberg, M. Balaz, *et al.* In vitro sliding of actin filaments labelled with single quantum dots. *Biochem. Biophys. Res. Commun.* 314:529–534, 2004. doi:10.1016/j.bbrc.2003.12.133.

61Mattoussi, H., A. W. Cumming, C. B. Murray, M. G. Bawendi, and R. Ober. Properties of CdSe nanocrystal dispersions in the dilute regime: structure and interparticle interactions. *Phys. Rev. B* 58:7850–7863, 1998. doi:10.1103/PhysRevB.58.7850.

62Mattoussi, H., J. M. Mauro, E. R. Goldman, G. P. Anderson, V. C. Sundar, F. V. Mikulec, and M. G. Bawendi. Self-assembly of CdSe–ZnS quantum dot bioconjugates using an engineered recombinant protein. *J. Am. Chem. Soc.* 122:12142–12150, 2000. doi:10.1021/ja002535y.

63Mattoussi, H., L. H. Radzilowski, B. O. Dabbousi, E. L. Thomas, M. G. Bawendi, and M. F. Rubner. Electroluminescence from heterostructures of organic PPV and inorganic nanocrystals. *J. Appl. Phys.* 83:7965–7974, 1998. doi:10.1063/1.367978.

64Medintz, I. L., A. R. Clapp, H. Mattoussi, E. R. Goldman, and J. M. Mauro. Nanoscale biosensor assemblies built on quantum dot FRET donors. *Nat. Mater.* 2:630–638, 2003. doi:10.1038/nmat961.

65Medintz, I. L., P. E. Dawson, A. R. Clapp, H. T. Uyeda, E. L. Chang, J. R. Deschamps, and H. Mattoussi. Monitoring protease activity using QD–peptide conjugates and energy transfer. *Nat. Mater.* 5:581–589, 2006. doi:10.1038/nmat1676.

66Medintz, I. L., J. H. Konnert, A. R. Clapp, I. Stanish, M. E. Twigg, H. Mattoussi, J. M. Mauro, and J. R. Deschamps. A fluorescence resonance energy transfer-derived structure of a quantum dot–protein bioconjugate nanoassembly. *Proc. Natl. Acad. Sci.* 101:9612–9617, 2004. doi:10.1073/pnas.0403343101.

67Medintz, I. L., H. T. Uyeda, E. R. Goldman, *et al.* Quantum dot bioconjugates for imaging, labelling and sensing. *Nat. Mater.* 4:435–446, 2005. doi:10.1038/nmat1390.

68Mei, B. C., K. Susumu, I. L. Medintz, J. B. Delehanty, and H. Mattoussi. Modular poly(ethylene glycol) ligands for biocompatible semiconductor and gold nanocrystals with extended pH and ionic stability. *J. Mater. Chem.* 18:4949–4958, 2008. doi:10.1039/b810488c.

69Michalet, X., F. F. Pinaud, L. A. Bentolila, J. M. Tsay, S. Doose, J. J. Li, G. Sundaresan, A. M. Wu, S. S. Gambhir, and S. Weiss. Quantum dots for live cells, in vivo imaging, and diagnostics. *Science* 307:538–544, 2005. doi:10.1126/science.1104274.

70Murray, C. B., C. R. Kagan, and M. G. Bawendi. Synthesis and characterization of monodisperse nanocrystals and close-packed nanocrystal assemblies. *Ann. Rev. Mater. Sci.* 30:545, 2000. doi:10.1146/annurev.matsci.30.1.545.

71Murray, C. B., D. J. Norris, and M. G. Bawendi. Synthesis and characterization of nearly monodisperse CdE (E = sulfur, selenium, tellurium) semiconductor nanocrystallites. *J. Am. Chem. Soc.* 115:8706–8713, 1993. doi:10.1021/ja00072a025.

72Murray, C. B., S. Sun, W. Gaschler, H. Doyle, T. A. Betley, and C. R. Kagan. Colloidal synthesis of nanocrystals and nanocrystal superlattices. *IBM J. Res. Dev.* 45:47–56, 2001.

73Nann, T. Phase-transfer of CdSe@ZnS quantum dots using amphiphilic hyperbranched polyethylenimine. *Chem. Commun.*, 1735–1736, 2005. doi:10.1039/b414807j.

74Nirmal, M., B. O. Dabbousi, M. G. Bawendi, J. J. Macklin, J. K. Trautman, T. D. Harris, and L. E. Brus. Fluorescence intermittency in single cadmium selenide nanocrystals. *Nature* 383:802–804, 1996. doi:10.1038/383802a0.

75Norris, D. J., A. Sacra, C. B. Murray, and M. G. Bawendi. Measurement of the size dependent hole spectrum in CdSe quantum dots. *Phys. Rev. Lett.* 72:2612, 1994. doi:10.1103/PhysRevLett.72.2612.

76Oh, E., D. Lee, Y. P. Kim, S. Y. Cha, D. B. Oh, H. A. Kang, J. Kim, and H. S. Kim. Nanoparticle-based energy transfer for rapid and simple detection of protein glycosylation. *Angew. Chem. Int. Ed.* 45:7959, 2006. doi:10.1002/anie.200601948.

77Park, J., J. J. Soon, G. Kwon, Y. Jang, and T. Hyeon. Synthesis of monodisperse spherical nanocrystals. *Angew. Chem. Int. Ed.* 46:4630–4660, 2007. doi:10.1002/anie.200603148.

78Pellegrino, T., L. Manna, S. Kudera, T. Liedl, D. Koktysh, A. L. Rogach, S. Keller, J. Radler, G. Natile, and W. J. Parak. Hydrophobic nanocrystals coated with an amphiphilic polymer shell: a general route to water soluble nanocrystals. *Nano Lett.* 4:703–707, 2004. doi:10.1021/nl035172j.

79Peng, X. G., M. C. Schlamp, A. V. Kadavanich, and A. P. Alivisatos. Epitaxial growth of highly luminescent CdSe/CdS core/shell nanocrystals with photostability and electronic accessibility. *J. Am. Chem. Soc.* 119:7019–7029, 1997. doi:10.1021/ja970754m.

80Peng, Z. A., and X. Peng. Formation of high-quality CdTe, CdSe, and CdS nanocrystals using CdO as precursor. *J. Am. Chem. Soc.* 123:183–184, 2001. doi:10.1021/ja003633m.

81Pinaud, F., D. King, H. P. Moore, and S. Weiss. Bioactivation and cell targeting of semiconductor CdSe/ZnS nanocrystals with phytochelatin-related peptides. *J. Am. Chem. Soc.* 126:6115–6123, 2004. doi:10.1021/ja031691c.

82Pinaud, F., X. Michalet, G. Iyer, E. Margaret, H.-P. Moore, and S. Weiss. *Traffic.* doi: 10.1111/j.1600-0854.2009.00902.x.

83Pons, T., I. L. Medintz, H. T. Uyeda, and H. Mattoussi. Spectrally-dependent fluorescence resonant energy transfer using quantum dot donors: ensemble and single molecule studies. *Phys. Rev. B* 73:245302, 2006. doi:10.1103/PhysRevB.73.245302.

84Pons, T., I. L. Medintz, X. Wang, *et al.* Solution-phase single quantum dot fluorescence resonance energy transfer. *J. Am. Chem. Soc.* 128:15324–15331, 2006. doi:10.1021/ja0657253.

85Pons, T., H. T. Uyeda, I. L. Medintz, and H. Mattoussi. Hydrodynamic dimensions, electrophoretic mobility and stability of hydrophilic quantum dots. *J. Phys. Chem. B* 110:20308–20316, 2006. doi:10.1021/jp065041h.

[86] Qu, L., Z. A. Peng, and X. Peng. Alternative routes toward high quality CdSe nanocrystals. *Nano Lett*. 1:333–337, 2001. doi:10.1021/nl0155532.

[87] Rajan, S. S., H. Y. Liu, and T. Q. Vu. Studying the molecular scale dynamics of receptor endocytic trafficking in live cells. *ACS Nano* 2:1153–1166, 2008. doi:10.1021/nn700399e.

[88] Rajan, S. S., and T. Q. Vu. Quantum dots monitor TrkA receptor dynamics in the interior of neural PC12 cells. *Nano Lett*. 6:2049–2059, 2006. doi:10.1021/nl0612650.

[89] Reiss, P., J. Bleuse, and A. Pron. Highly luminescent CdSe/ZnSe core/shell nanocrystals of low size dispersion. *Nano Lett*. 2:781–784, 2002. doi:10.1021/nl025596y.

[90] Rossetti, R., J. E. Ellison, J. M. Gibson, and L. E. Brus. Size effects in the excited electronic states of small colloidal CdS crystallites. *J. Chem. Phys*. 80:4464–4469, 1984. doi:10.1063/1.447228.

[91] Saxton, M., and K. Jacobson. Single-particle tracking: applications to membrane dynamics. *Annu. Rev. Biophys. Biomol. Struct*. 26:373, 1997. doi:10.1146/annurev.biophys.26.1.373.

[92] Seitz, A., and T. Surrey. Processive movement of single kinesins on crowded microtubules visualized using quantum dots. *EMBO J*. 25:267–277, 2006. doi:10.1038/sj.emboj.7600937.

[93] Shi, L. F., V. De Paoli, N. Rosenzweig, and Z. Rosenzweig. Synthesis and application of quantum dots FRET-based protease sensors. *J. Am. Chem. Soc*. 128:10378–10379, 2006. doi:10.1021/ja063509o.

[94] Snee, P. T., R. C. Somers, G. Nair, J. P. Zimmer, M. G. Bawendi, and D. G. Nocera. A ratiometric CdSe/ZnS nanocrystal pH sensor. *J. Am. Chem. Soc*. 128:13320–13321, 2006. doi:10.1021/ja0618999.

[95] Somers, R. C., M. G. Bawendi, and D. G. Nocera. CdSe nanocrystal based chem-/bio-sensors. *Chem. Soc. Rev*. 36:579–591, 2007. doi:10.1039/b517613c.

[96] Susumu, K., B. C. Mei, and H. Mattoussi. Multifunctional ligands based on dihydrolipoic acid and polyethylene glycol to promote biocompatibility of quantum dots. *Nat. Protocols* 4:424–436, 2009. doi:10.1038/nprot.2008.247.

[97] Susumu, K., H. T. Uyeda, I. L. Medintz, T. Pons, J. B. Delehanty, and H. Mattoussi. Enhancing the biological stability and functionalities of quantum dots via compact multifunctional surface ligands. *J. Am. Chem. Soc*. 129:13987–13996, 2007. doi:10.1021/ja0749744.

[98] Ueda, M., Y. Sako, T. Tanaka, P. Devreotes, and T. Yanagida. Single-molecule analysis of chemotactic signaling in dictyostelium cells. *Science* 294:864, 2001. doi:10.1126/science.1063951.

[99] Uyeda, H. T., I. L. Medintz, J. K. Jaiswal, S. M. Simon, and H. Mattoussi. Synthesis of compact mutidentate ligands to prepare stable hydrophilic quantum dot fluorophores. *J. Am. Chem. Soc*. 127:3870–3878, 2005. doi:10.1021/ja044031w.

[100] Wang, M., N. Felorzabihi, G. Guerin, J. C. Haley, G. D. Scholes, and M. A. Winnik. Water-soluble CdSe quantum dots passivated by a multidentate diblock copolymer. *Macromolecules* 40:6377–6384, 2007. doi:10.1021/ma070553v.

[101] Wang, Y. A., J. J. Li, H. Chen, and X. Peng. Stabilize inorganic nanocrystals by organic dendrons. *J. Am. Chem. Soc*. 124:2293–2298, 2002. doi:10.1021/ja016711u.

[102] Warshaw, D. M., G. G. Kennedy, S. S. Work, *et al*. Differential Labeling of myosin V heads with quantum dots allows direct visualization of hand-over-hand processivity. *Biophys. J*. 88:L30–L32, 2005. doi:10.1529/biophysj.105.061903.

[103] Wehrenberg, B. L., C. Wang, and P. Guyot-Sionnest. Interband and intraband optical studies of PbSe colloidal quantum dots. *J. Phys. Chem. B* 106:10634–10640, 2002. doi:10.1021/jp021187e.

[104] Wu, X., H. Liu, J. Liu, K. N. Haley, J. A. Treadway, J. P. Larson, N. Ge, F. Peale, and M. P. Bruchez. Immunofluorescent labeling of cancer marker Her2 and other cellular targets with semiconductor quantum dots. *Nat. Biotechnol*. 21:41–46, 2003. doi:10.1038/nbt764.

[105] Xie, R. G., U. Kolb, J. X. Li, T. Basche, and A. Mews. Synthesis and characterization of highly luminescent CdSe–core CdS/$Zn_{0.5}Cd_{0.5}$S/ZnS multi-shell nanocrystals. *J. Am. Chem. Soc*. 127:7480–7488, 2005. doi:10.1021/ja042939g.

[106] Xie, X. S., and J. K. Trautman. Optical studies of single molecules at room temperature. *Ann. Rev. Phys. Chem*. 49:441–480, 1998. doi:10.1146/annurev.physchem.49.1.441.

[107] Yao, J., D. R. Larson, H. D. Vishwasrao, *et al*. Blinking and nonradiant dark fraction of water-soluble quantum dots in aqueous solution. *Proc. Natl. Acad. Sci*. 102:14284–14289, 2005. doi:10.1073/pnas.0506523102.

[108] Yildiz, A., J. N. Forkey, S. A. McKinney, T. Ha, Y. E. Goldman, and P. R. Selvin. Myosin V walks hand-over-hand: single fluorophore imaging with 1.5-nm localization. *Science* 300:2061–2065, 2003. doi:10.1126/science.1084398.

[109] Yu, W. W., E. Chang, J. C. Falkner, J. Zhang, A. M. Al-Somali, C. M. Sayes, J. Johns, R. Drezek, and V. L. Colvin. Forming biocompatible and nonaggregated nanocrystals in water using amphiphilic polymers. *J. Am. Chem. Soc*. 129:2871–2879, 2007. doi:10.1021/ja067184n.

[110] Yu, W. W., J. C. Falkner, B. S. Shih, and V. L. Colvin. Preparation and characterization of monodisperse PbSe semiconductor nanocrystals in a noncoordinating solvent. *Chem. Mater*. 16:3318–3322, 2004. doi:10.1021/cm049476y.

[111] Zhang, C. Y., and L. W. Johnson. Quantum dot-based fluorescence resonance energy transfer with improved FRET efficiency in capillary flows. *Anal. Chem*. 78:5532–5537, 2006. doi:10.1021/ac0605389.

[112] Zhang, C. Y., and L. W. Johnson. Microfluidic control of fluorescence resonance energy transfer: breaking the FRET limit. *Angew. Chem. Int. Ed*. 46:3482–3485, 2007. doi:10.1002/anie.200604861.

[113] Zhang, C. Y., and L. W. Johnson. Quantifying RNA–peptide interaction by single-quantum dot-based nanosensor: an approach for drug screening. *Anal. Chem*. 79:7775–7781, 2007. doi:10.1021/ac071225w.

[114] Zhang, C. Y., H. C. Yeh, M. T. Kuroki, *et al*. Single-quantum-dot-based DNA nanosensor. *Nat. Mater*. 4:826–831, 2005. doi:10.1038/nmat1508.

[115] Zhang, Q., Y. Li, and R. W. Tsien. The dynamic control of kiss-and-run and vesicular reuse probed with single nanoparticles. *Science* 323:1448–1453, 2009. doi:10.1126/science.1167373.